Modelling car-following behaviour of connected vehicles with a focus on driver compliance

Anshuman Sharma[a], Zuduo Zheng[a,1], Ashish Bhaskar[b], Md. Mazharul Haque[b]

[a]*School of Civil Engineering, The University of Queensland, St. Lucia 4072, Brisbane, Australia*
[b]*School of Civil Engineering and Built Environment, Science and Engineering Faculty, Queensland University of Technology (QUT), 2 George St, Brisbane, Qld. 4001, Australia*

Abstract

This paper incorporates the driver compliance behaviour into a connected vehicle driving strategy (CVDS) that can be integrated with traditional car-following (CF) models to better describe the connected vehicle CF behaviour. Driver compliance, a key human factor for the success of connected vehicles technology, is modelled using a celebrated theory of decision making under risk – the Prospect theory (PT). The reformulated value and weighting functions of PT are consistent with the driver compliance behaviour and also preserve the integral elements of PT. Furthermore, the connected vehicle trajectory data collected from a carefully designed advanced driving simulator experiment are utilised to calibrate CVDS integrated with Intelligent Driver Model (IDM), i.e., CVDS-IDM. The calibration results reveal that drivers in the connected environment drive safely and efficiently. Moreover, the CVDS-IDM can successfully model and predict the CF dynamics of connected vehicles and is more behaviourally and numerically sound than a traditional CF model.

Keywords: Driver compliance; Prospect theory; Human factors; Connected vehicles; Car-following; Intelligent Driver Model (IDM)

1. INTRODUCTION

Human factors are often disregarded in traffic flow models which has made them insufficient for explaining the complex interactions between the human drivers and some important resulting traffic flow phenomena. More specifically, CF models that are based on the laws of physics have been criticised for their inability in explaining human driving behaviours during CF. Incorporating human factors in CF models can assist in explaining driving behaviour in various driving conditions, such as traffic breakdowns, traffic oscillations, driver risk-taking behaviours, distraction, and adverse weather conditions (refer Saifuzzaman and Zheng (2014) for a review of CF models from engineering and human factors perspective). Moreover, CF models capable of mimicking driver errors and ability to generate crash or near-crash scenarios can be important tools for evaluating traffic safety (Laval et al., 2014; Saifuzzaman et al., 2015). Overall, incorporating human factors in CF models would enable us to holistically investigate traffic modelling, control, and safety, etc.

---

[1] Corresponding author. Tel.: +61 7 3443 1371
E-mail address: zuduo.zheng@uq.edu.au (Z. Zheng)

The success of connected vehicle technology will heavily rely on the driver compliance with the transmitted information (Sharma et al., 2017). When the information is provided to a driver, he/she can either act according to the information or completely (or partially) ignore it, e.g., in response to a warning about the leading vehicle braking hard, the driver (follower) can either brake if he/she has noticed the warning, or responds only after noticing the leader's braking if he/she has ignored the warning. Intuitively, the latter case nullifies the advantages of connected vehicle technology. Therefore, understanding and modelling of the driver compliance behaviour are imperative tasks before the wide-scale deployment of connected vehicle technologies.

Recently, notable efforts have been made on modelling connected vehicle car-following (CVCF) behaviour (Ge and Orosz, 2014; Jia and Ngoduy, 2016; Li and Qiu, 2018; Mittal et al., 2017; Monteil et al., 2014; Ni et al., 2011; Rahman et al., 2018; Talebpour et al., 2017, 2016; Tang et al., 2014). These CVCF models can be broadly classified as event-driven models, continuous models, and psychophysical models. Event-driven models assume that driving behaviour in the connected environment (CE) changes only when the audio or the video feedback (warnings or advice) provides an alert for potentially hazardous events such as accidents or hard braking by the lead vehicle, e.g., the model by Tampere et al. (2009). Continuous models assume a perpetual change in driving behaviour when the audio or video feedback is continuously presented to the driver, e.g., the models discussed in Talebpour et al. (2016); Talebpour and Mahmassani (2016); Tang et al. (2014); and Zhu and Ukkusuri (2017).

Similar to most of the CF models for traditional vehicles, the aforementioned CVCF models also assume that the driver reacts towards arbitrarily small changes in the relative speed (or other stimulus). Particularly, the CF models above assume that the driver fully complies with the information provided. These models, thus, completely ignore human factors such as driver compliance. Arguably, human factors will play a major and a predominant role in governing the CVCF dynamics. Psychophysical models are capable of incorporating those human factors that influence the driver's decision-making in various driving situations plausible in the CE. A few notable attempts made in the literature are as follows: Ni et al. (2011) assumed different perception-reaction time distributions for information assisted and information unassisted drivers, whereas Jia et al. (2012) developed psychophysical model with CF suggestions considering various perception thresholds, such as minimum desired following distance, minimum desired stopping distance, and threshold of relative speed among others.

In the aforementioned studies, a common and perhaps the most critical gap identified is the ignorance or inadequate consideration of the driver compliance and its influence on CF behaviour. In addition, a few studies directly adopted the existing CF models in their original form to model the CVCF behaviour even without examining the models' suitability. Previous studies relied on numerical experiments or employed trajectories of traditional vehicles to calibrate CF models by imposing some strong assumptions, and did not calibrate their developed models using connected vehicle (CV) trajectory data due to the paucity of such data. Therefore, the following important questions are still largely unexplored: (a) what changes are expected in the CF behaviour due to a CE? (b) are traditional CF models capable of describing

the CVCF behaviour? If not, (c) how to incorporate the driver compliance behaviour in CF models to better mimic the CVCF behaviour?

Motivated by the research needs above, this study aims to incorporate driver compliance using a general connected vehicle driving strategy (CVDS) that can be integrated with traditional CF models. Driver compliance behaviour, which is a typical case of decision making under risk (explained later), is modelled using the celebrated Prospect Theory (PT). To overcome the unavailability of CV data, a driving simulator experiment has been carefully designed and conducted to collect the CV trajectory data necessary for developing and testing the CVDS. The trajectory data are collected for two scenarios: baseline (without any information assistance) and connected (with certain types of information assistance). In this paper, a widely adopted CF model i.e., Intelligent Driver Model (IDM) (Treiber et al., 2000) is used to demonstrate how CVDS can be integrated with a traditional CF model and how the integrated model (CVDS-IDM) performs through rigorous calibration. By doing so, the paper sheds light on how a CE can influence CF behaviour, and demonstrates the superiority of CVDS-IDM over a traditional CF model in describing the CVCF behaviour.

The remainder of the paper is organised as follows. Section 2 describes the driving simulator experiment design in detail. Section 3 presents PT-based modelling of the driver compliance behaviour. Section 4 discusses the CVDS and its integration with IDM (i.e., CVDS-IDM), and Section 5 details the methodology to calibrate CVDS-IDM. Section 6 presents the results and discusses the behavioural and numerical soundness of the CVDS-IDM. Finally, Section 7 summarises the main conclusions and suggests future research directions.

2. CONNECTED VEHICLE DATA COLLECTION

The unavailability of real-world CV data is a big challenge for researchers to develop, calibrate and validate the CVCF models. There are a number of pilot projects currently around the world including the U.S., Europe, South Korea, Japan, China, Australia, and etc. Emami et al. (2018) have published a good review of these testbeds and others. To the best of our knowledge, no investigation has been made towards human factor considerations in CF scenarios in a connected vehicle environment. Thus, in this research, a driving simulator experiment was designed and conducted to collect the necessary CV trajectory data with a focus on human factors. This section details the driving simulator experiment design. Please note that this driving simulator experiment was designed for a project with a larger scope and only the part relevant to this study is presented below.

2.1 The driving simulator

The CARRS-Q Advanced Driving Simulator is a high-fidelity simulator that consists of a complete car with working controls. The simulator is attached with eight computers, projectors, and a rotating base with the capability to move and rotate in three directions (6 degrees of freedom). Furthermore, the simulator can reproduce high-resolution real-world scenarios in a virtual environment on 180º field of view (e.g., actual sound effects of the engine, car-road interactions, passing by traffic, etc.). The simulator utilizes SCANeR™ studio software that

couples vehicle dynamics with virtual road environment, and displays road environment and traffic interactions on front projectors, rear-view mirrors, and wing mirrors at a rate of 60 Hz. For further information refer to CARRS-Q (2018) and Haque and Washington (2015).

2.2 Experiment design

Participants are required to drive the simulator car in the baseline and connected scenarios. Note that the baseline scenario refers to traditional environment i.e., traffic environment consisting of vehicles without any communication capability whereas connected scenario mimics the future CE consisting of vehicles with communication capability and the uninterrupted dissemination of information. Each participant has to follow a platoon of vehicles on a single-lane motorway for 3 km in each scenario. Figure 1(a) displays the road geometry. Hereon, the simulator car driven by a participant is termed as 'driven car', the vehicle immediately in front of the simulator car (the first leader) is termed as 'leading car' (see Figure 1(b)), and the platoon of vehicles in front of the simulator car is termed as 'leading cars'. Moreover, participants were able to see up to two vehicles ahead to capture the multivehicle anticipation. The second leader was a mini truck which was clearly visible at all the time. In the baseline scenario, the participants drive the simulator car without driving aids, while in the connected scenario, to simulate V2V and V2I information dissemination the participants are assisted with driving aids displayed on the windscreen of the simulator car. Figure 1(c) depicts the participant's view.
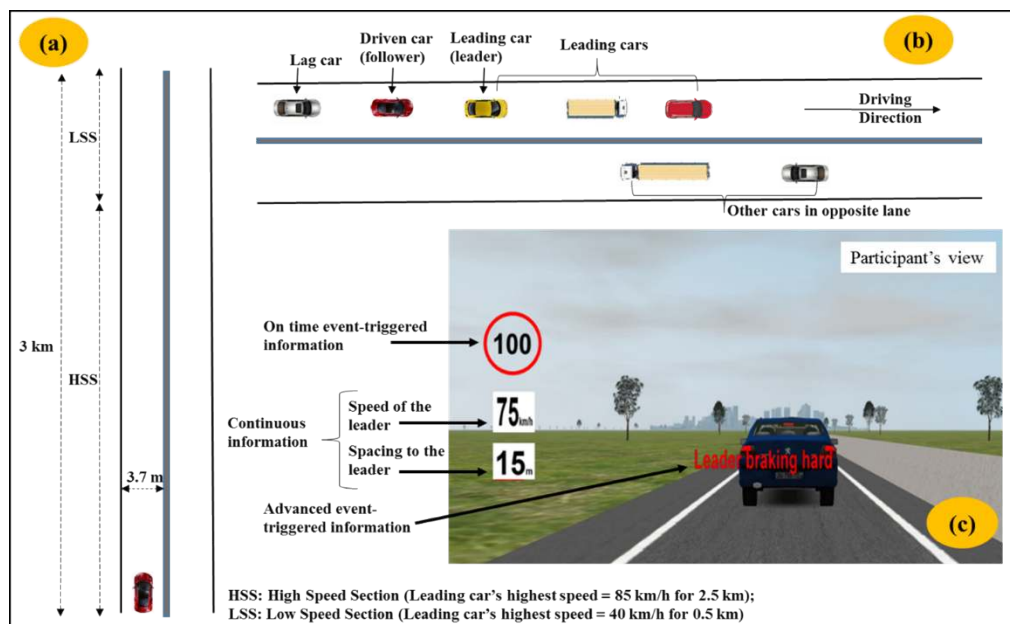
Figure 1 Details of the driving simulator experiment. (a) The road geometry; (b) The vehicles in the simulator environment; (c) Categories of the information available in the connected scenario.

To ensure the realism of the participants' driving experience using the driving simulator, the experiment has been meticulously designed by providing a realistic driving environment and driving scenarios. Several effective strategies have been carefully implemented to minimize any potential learning effect, e.g., the randomised sequence of the drives, different driving

environment and surrounding traffic in each drive, a break between the drives, etc. For more information, see Ali et al. (2018).

2.2.1 Connectivity design

Driving aids are cautiously designed after a comprehensive review of the literature on in-vehicle driver assistance systems and the current driving aids provided by major car manufacturers. In the ensuing paragraphs, we describe the type of information provided and how it is presented.

In the connected scenario, two categories of information (driving aids) are provided to a participant: a) continuous information; and b) advanced event-triggered information. Continuous information is always available to the participants, including the leading car's speed, and the spacing between the driven and leading cars. Assuming that the connectivity technologies will be smart enough to warn the drivers in advance, advanced event-triggered information 'leader braking hard' is also delivered to the participants 3 seconds before the leading car actually brakes hard. We believe connectivity can enhance the capabilities of systems like RECAS (Lee et al., 2002) and CLEWS (Greene et al., 2011), thereby making reliable and efficient advanced event-triggered information possible. To comprehend the rationale behind providing advanced event-triggered information, let's picture a scenario in which a vehicle follows 3 leaders (same as Figure 1 of the revised manuscript, v1-> v2 ->v3->v4) and all vehicles are in CF regime. After some time, the first leader (v4) brakes hard. In TE, following vehicles will brake one after the other, and in most cases, a vehicle (say v1) will brake only after observing the brake of the vehicle that is immediately in front (v2). Multivehicle anticipation also plays a role in followers' responses but majorly a follower responds to the vehicle immediately in front. In TE, we can expect that if the vehicle v4 starts braking at 't' seconds then v1 will commence the braking at around 't + Δt' seconds, where Δt represents the time taken by v1 to react to v2's speed reduction. In CE, vehicles receive information about surrounding vehicles' actions and in this case leaders' actions. As soon as v4 starts braking each of the 3 vehicles will receive the warning message 'leader braking hard' at almost the same time (assuming negligible communication delay). For the vehicle v3, the information will be an on-time event triggered by v4's braking; however, for v1 it will be an advanced event since v2 has not started braking yet when v1 receives such message. How early such message will be delivered to v1 can vary as per the design of the connectivity (i.e., communication type, range, etc.) and the length of the platoon. In our driving simulator experiment, we have incorporated this advanced information condition among other conditions and have recorded drivers' responses.

The next natural question is why the message is delivered 3 seconds in advance? On average, drivers take 2 s to respond to a stimulus. In order to ensure that the full impact of connectivity in assisting drivers' decision making can be captured, we have provided additional 1 s to cater for the time needed for perceiving and understanding the text message displayed on the screen. Also, in our pilot testings, we tested different time windows, i.e., 2.5, 3, and 4 s, and observed that 4 s was too long while 2.5 s was insufficient for many participants. Thus, we eventually adopted 3 s in the final experiment.

An effective driving aid design balances the method of information presentation and the amount of screen time. The literature reflects that researchers have mainly adopted three types

of information presentation namely, auditory (Ben-Yaacov et al., 2002; Groeger, 1998; Maltz and Shinar, 2007), imagery (Comte and Jamson, 2000; Erke et al., 2007; Saffarian et al., 2013), or both (Adell et al., 2011; Fairclough et al., 1997; Ghadiri et al., 2013; Lee et al., 2002; May et al., 1995). The auditory information is conveyed using either a beep sound or a voice message while the imagery information is presented either by displaying an image or through a text message.

Table 1 Categories of information: types of events, corresponding messages, and their presentation style.

Categories of information	Type of event	Message trigger point	Information presentation		
			Text/Image (example)	Time duration on the windscreen	Audio
Continuous information	Following the leading car	Leading car speed at every instant	**75**km/h	Always	-
		Spacing to leading car at every instant	**15**m	Always	-
Advanced event-triggered information	Leading car braking hard	3 sec before leading car brakes hard	**Leader Braking Hard**	3 sec	3 beeps (one by one)

We adopted a combination of both the audio and imagery presentations to disseminate the information. All the text messages, e.g., 'leader braking hard' are projected on the screen for 3 seconds accompanied with three beep sounds (one beep per second). All the warning symbols, e.g., 'Speed limit sign' are encircled with a red boundary accompanied with one beep sound. Table 1 summarises the characteristics of all the driving aids.

2.2.2 Vehicle interaction design

The vehicular interactions are designed such that drivers undergo all the driving regimes transitions, which leads to a dataset containing complete trajectories. A trajectory is complete if it constitutes all the six driving regimes, i.e., free acceleration, cruising at the desired speed, following the leader at a constant speed, accelerating behind a leader, decelerating behind a leader, and standing behind a leader (Sharma et al., 2018a). Completeness of the driving regimes is an important aspect of the trajectory data quality and critical for the purpose of CF model calibration and validation. Treiber and Kesting (2013a) have empirically demonstrated the importance of trajectory completeness on model calibration. Punzo et al. (2015) demonstrated that the variance of the simulation error is lower for longer trajectories than for shorter ones, thereby indicating that longer trajectories including different driving regimes (car-following and free-flow) have to be preferred for model calibration. Furthermore, Sharma et al. (2018a) proposed a pattern recognition algorithm for vehicle trajectories (PRAVT) to automatically and accurately identify different driving regimes in vehicle trajectory data, and

Sharma et al. (2018b) concluded that the average calibrated parameters obtained from the complete trajectories perform better in validation with smaller validation errors. As mentioned before, a single lane divided highway is considered in this study. An important reason to prefer the single lane divided motorway is to ensure that no lateral movements (lane change manoeuvres) occur at all the time. A lane change manoeuvre is undesired since the primary objective is to observe drivers' CF behaviour in a CE and collect the corresponding data. In addition, given the extent of CF interactions (complete trajectories, and high-speed and low speed sections) this research aim to observe, the complexities involved in designing these interactions and collecting the data, and the peculiarity of drivers' behaviour when interacting with messages provided in CE, we restrict the scenario to single lane divided motorways.

Figure 2 shows the speed profile of the leading car depicting the high-speed and the low-speed CF regions. At the beginning of CF, the leading cars, the driven car, and the lag car are at standstill (Figure 1(b)). The leading cars start accelerating and continue to accelerate until they attain a speed of 23.5 m/s (85 km/h), and maintain this speed for 50 s. After the driven car starts accelerating, the lag car also accelerates and maintains a fixed distance from the driven car. Next, the leading cars decelerate hard to mimic the hard braking and arrive at a standstill. After 5 s, the leading cars go through the same cycle of acceleration, constant speed, hard deceleration, and standstill, although this time, the constant speed maintained is 11 m/s (40 km/h), much smaller than the previous constant speed in order to create a low-speed CF region. Note that the vehicle interactions remain the same in the baseline and in the connected scenario.
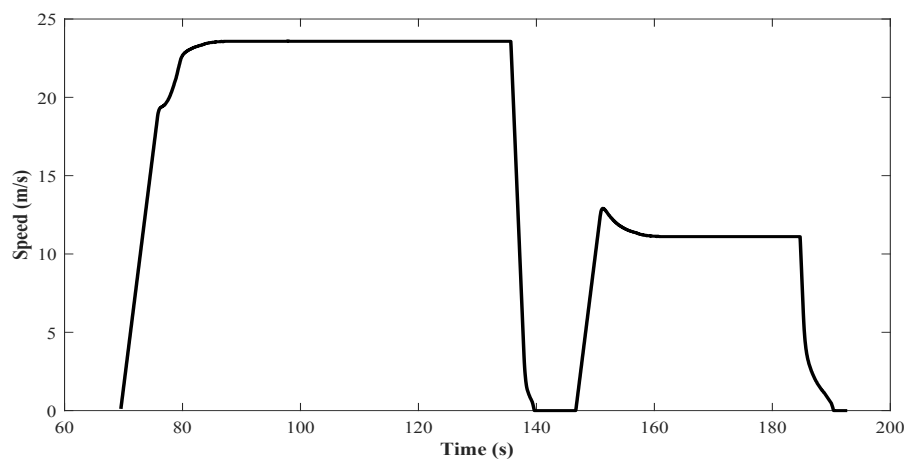
Figure 2 Speed profile of the leading car.

2.3 Participants

Seventy-eight eligible participants were recruited. A participant is eligible if he/she is between 18 to 65 years old, holds either a provisional or an open Australian driving licence, has no history of motion sickness or epilepsy, and is not pregnant. Participants received AU $75 as compensation of their time.

The average age of the participants is 30.8 years with a standard deviation of 11.7 years. Out of 78 participants, 34.9% are female and 61.6% have a university degree. Overall, the participants have a diverse background and the data collected from the experiments have a

reasonable representation of drivers with different sociodemographic background. A detailed note on participant testing protocol is reported elsewhere (Ali et al., 2018).

This study utilises all the 78 leader-follower trajectory pairs from the baseline and connected scenarios (156 pairs in total). For the rest of the paper, the terms 'leader' and 'follower' denote the first leading car and the simulator car driven by a participant, respectively.

3. MODELLING DRIVER COMPLIANCE BEHAVIOUR USING PROSPECT THEORY

In this study, driver compliance is measured based on the driver's response when the information is presented and the compliance is divided into two levels (i.e., low and high compliance).

A driver's compliance decision to a warning message (e.g., 'leader braking hard') is a typical case of a decision under risk (risk of rear-end collision). Decision making under risk is frequently modelled by Expected Utility Theory (EUT) (von Neumann and Morgenstern, 1944) or Prospect Theory (Kahneman and Tversky, 1979). Here, prospect theory (PT) is employed since it is capable of describing rational and irrational driving behaviours observed in the real world in a realistic and consistent manner, as elaborated below. In 1992, Tversky and Kahneman (Tversky and Kahneman, 1992) published a generalised version of prospect theory called as cumulative prospect theory (abbreviated as cumulative PT) that is typically preferred in economic analysis. We adopt the same to model driver compliance behaviour.

Firstly, a driver's decision (e.g., travel speed, behavioural pattern, etc.) can be rational as well as irrational because his/her decisions are driven by personality, psychological state, risk preference, environmental factors, etc. (Atzwanger and Ruso, 2004; Dia, 2002; Summala, 1988). EUT is most suitable for modelling the rational decision makers while PT can capture both rational and irrational decision-making mechanisms. Meanwhile, PT assumes that decision-makers value the choices in terms of gains and losses measured relative to some reference point and not on the final gain as in the case of EUT. Such reference dependence fits characteristics of drivers' decision makings in CF because a driver's decision to accelerate or decelerate at time $(i + 1)$ is dependent on his/her state variables (e.g., speed, spacing, relative speed etc.) at time (i).

Additionally, we also demonstrate later how four integral elements of PT (i.e., reference dependence, loss aversion, diminishing sensitivity, and probability weighting) can consistently describe the key characteristics of a driver compliance behaviour.

3.1 Prospect Theory – a brief introduction

PT, developed by Kahneman and Tversky (1979), is a behavioural economic theory that explains how individuals evaluate risks and make choices between risky probabilistic alternatives. PT can be applied to prospects that are uncertain as well as risky. In PT, a decision maker associates a perceived utility with each of the available choices and chooses the one with the maximum perceived utility. PT has been studied and applied in different disciplines, e.g.,

economics (Barberis and Huang, 2008), political science (Levy, 2003), health (Attema et al., 2013), and law (Guthrie, 2002), etc. In Transportation Engineering, PT is predominantly applied to model the route choice behaviour (Avineri and Bovy, 2008; Avineri and Prashker, 2004; Gao et al., 2010; Xu et al., 2011; Yang and Jiang, 2014) and rarely used to model the CF behaviour with the exception of the work by Hamadar and his collaborators (Hamdar et al., 2008, 2015; Talebpour et al., 2011). To the best of the authors' knowledge, PT has never been applied to model the driver compliance behaviour in a CE.

To mimic or predict the choice of a decision maker using PT, first, prospects are identified and formulated (outcomes are assigned corresponding to each prospect). Note that choices given to the decision maker are termed as prospects in PT. Next, utility values are calculated for each prospect. The prospect with maximum utility depicts the final choice of the decision maker. Consider a case where a commuter makes a choice between two alternative bus stops, A and B that have different bus headway distributions to reach the desired destination. We need to model this decision making using PT. When applying PT, each bus stop serves as a prospect. Next, the prospects are formulated i.e., possible gains/losses with their objective probabilities are assigned to each prospect. In this case, prospects are formulated in terms of possible waiting times of the commuter at each bus stop with corresponding probabilities. After this utility values are calculated for prospects and as per PT, the decision maker will choose the prospect i.e., the bus stop having the maximum utility. Refer to Avineri (2004) for an empirical example.

Consider a prospect f given by $(x_{-m}, p_{-m}; x_{-m+1}, p_{-m+1}; ....; x_0, p_0; ....; x_{n-1}, p_{n-1}; x_n, p_n)$ read as "outcome (amount of gain/loss) x_{-m} with probability p_{-m}, outcome x_{-m+1} with probability p_{-m+1} and so on." The outcomes are arranged in increasing order such that $x_i < x_j$ for $i < j$, and where $x_0 = 0$. The utility associated with the prospect f as per cumulative PT is presented in Equation (1):

$$U(f) = \sum_{i=-m}^{n} \pi_i v(x_i) \tag{1}$$

where $v(\cdot)$ is the value function that assigns a value to an outcome x_i and π_i is the decision weight. A decision maker does not weigh outcomes by their objective probabilities but rather by transformed probabilities or decision weights. The decision weights are computed with the help of a weighting function whose argument is an objective probability i.e., $w(p_i)$. A simple prospect entails only two outcomes (a) Gain/Loss denoted by x and (b) Neutral denoted by 0. These gain, loss, and neutral are measured from the reference. A gain implies some positive or favourable addition to the decision maker's current situation, a loss implies some negative or unfavourable addition to the decision maker's current situation, and a neutral implies no change in the decision maker's current situation. Moreover, simple prospects are consistent with both the original and the cumulative versions of PT. The utility associated with a simple prospect denoted by (x, p) i.e., x with probability p and 0 with probability $1 - p$, respectively, is a product of value associated with x and weight according to p as shown in Equation (2):

$$U(x, p) = v(x)w(p) \tag{2}$$

Note that in PT $v(0) = 0$. The mathematical formulations of both $v(x)$ and $w(p)$ are shown in Equations (3) and (4):

$$v(x) = \begin{cases} x^\alpha & if \ x > 0 \\ -\lambda(-x)^\beta & if \ x \leq 0 \end{cases} \tag{3}$$

$$w(p) = \frac{p^\gamma}{(p^\gamma + (1-p)^\gamma)^{1/\gamma}} \tag{4}$$

where α, λ and γ are PT parameters that control the shape of the curves. The functions $v(x)$ and $w(p)$ are the value and the weight that the decision maker associates with the outcome x and its probability p, respectively. Note that $w(p)$ in Equation (4) is the weighting function for gains. The weighting function for losses has the same mathematical form with a different shape parameter i.e., replace γ in Equation (4) by δ. Figure 3 shows $v(x)$ and $w(p)$ curves as per Tversky and Kahneman (1992).
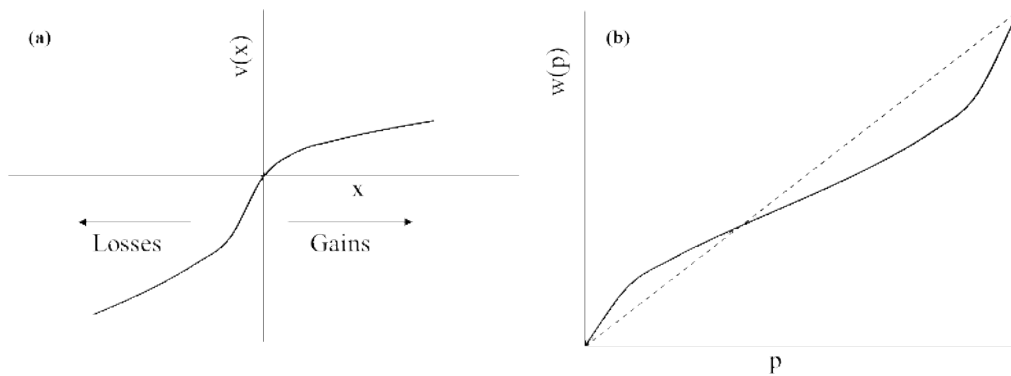

Figure 3 (a) The value function and (b) The weighting function.

As stated earlier, PT has four integral elements: a) reference dependence; b) loss aversion; c) diminishing sensitivity; and d) probability weighting. The first three elements are captured by the $v(x)$ and the last element by $w(p)$. More specifically, reference dependence manifests that a decision maker derives his/her utility from gains and losses measured from a reference point rather than an absolute value. Loss aversion explains that decision makers are more sensitive to losses than gains, and it is captured by making the loss part of the value function steeper ($\lambda > 1$) than the gain part (Figure 3(a)). Also, decision makers' sensitivity usually diminishes for large values of gains and losses. Such diminishing sensitivity is also reflected in the shape of $v(x)$: it has a concave shape for gains ($\alpha \leq 1$) and convex for losses ($\beta \leq 1$) as shown in Figure 3(a). Finally, probability weighting describes how a decision maker perceives probabilities and is quantified by Equation (4), e.g., smaller probabilities tend to be overweighted. It is easy to see from Equation (4) that when $\gamma = 1$, the probability weighting becomes linear as in EUT (the dashed line in Figure 3(b)). A decision maker is risk-seeking for small-probability gains and large-probability losses, and risk-aversion for small-probability losses and large-probability gains. For a detailed discussion on these four elements, see Kahneman and Tversky (1979) and Tversky and Kahneman (1992).

3.2 Driver compliance modelling based on Prospect Theory

It is reasonable to assume that all changes in driving behaviour (see Section 6) due to CE are attributed to the degree of driver compliance with information (high or low compliance). A zero compliance will lead to no change in CF behaviour in CE. All the factors such as trust in the connected vehicle technology, user acceptance of the technology, driver aggressiveness, and even the level of risk will ultimately influence the driver compliance. Furthermore, it is reasonable to assume that the driver's choice of the compliance generally depends on the time headway (hereon headway) at the time of information display. As headway decreases, drivers comply more and vice versa. Intuitively as well, a driver is more likely to comply high when an emergency message (advanced event-triggered message - 'leader braking hard') is delivered at small headway.

3.2.1 Compliance utility calculation

The compliance of a driver in response to the information is categorised as low compliance or high compliance levels. The two levels can be understood as two choices in front of a driver, the decision maker. To capture the subtle changes in the driver compliance, it is important to divide it into two levels. Moreover, different levels provide opportunities to characterise drivers, observe and learn differences in their behaviour, and understand how the drivers with different compliance level impact traffic flow. Furthermore, since the 3 PT parameters are sufficient to model the two categories of driver compliance levels, the two levels do not penalise in terms of model complexity. After perceiving and understanding the displayed information, the driver chooses one compliance level and responds accordingly. In this study, we are modelling this decision making using PT. The two compliance levels (low compliance and high compliance) are the two prospects and using PT we mimic which prospect i.e. compliance level, is chosen by the driver. The present treatment towards formulating these prospects is confined to simple prospects i.e., both prospects are simple prospects. Note that, in CF, any level of compliance (low or high) to a message displayed to assist the driver (e.g., warning message in an emergency) will represent a gain for the driver and complete ignorance of the message will represent a loss. Hence, both simple prospects are made up of gains. Obviously, the magnitude of gains at different compliance level will be different.

In line with utility formulation for simple prospects (Equation (2)), this study defines the compliance level utility as a product of usefulness and weight ($Compliance\ utility = usefulness \times weight$). The usefulness denotes how useful an information is to a driver, whereas the weight denotes how much a driver weighs the information at different compliance levels. Usefulness value is calculated using usefulness value function (similar to PT value function) and weights are calculated using weighting functions (similar to PT weighting function). Below we explain both usefulness value function and weighting function.

3.2.2 Usefulness value function

Since compliance utility is directly proportional to the usefulness, it is safe to assume that usefulness shares the same inverse proportionality relationship with observed headway as does the compliance. The smaller the observed headway is (at the time of information display), the

more useful the information is to the driver, and vice versa, e.g., an emergency message deliver at small headway is more useful to drivers. Moreover, in general, a logistic function is preferred when modelling choices (see the vast literature on discreet choice modelling, e.g., Hensher et al. (2015), Train (2009), etc.). Based on this and considering the properties of PT's value function, the usefulness value function is formulated as in Equation (5):

$$V\left(h_{obs}\right) = \frac{1}{\left(1 + e^{\lambda(\alpha h_{obs} - 1)}\right)} \tag{5}$$

where λ and α are the parameters that govern the shape of the function, and h_{obs} is the observed headway at a given time.
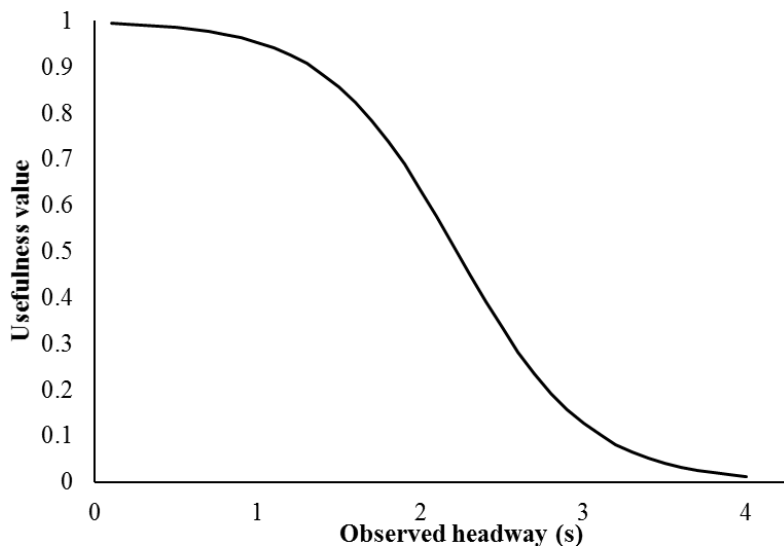

Figure 4 Usefulness value function plot ($\lambda = 5, \alpha = 0.4$)

Figure 4 depicts the inverse proportionality between the observed headway and the usefulness value as assumed previously. The sensitivity of usefulness value also diminishes for small and large headways, thus capturing the diminishing sensitivity property of PT. Furthermore, using the value function, one can estimate h_{max} (the headway when $V\left(h_{obs}\right)$ value is close to zero, which indicates the information is not useful at all) and h_{min} (the headway when $V\left(h_{obs}\right)$ value is close to one, which indicates the information is very useful). The headways h_{max} and $h_{min}$are later utilised to calculate weighting functions. In this study, the h_{max} is calculated at $V\left(h_{obs}\right)$ = 0.001 and h_{min} is calculated at $V\left(h_{obs}\right)$ = 0.99. The h_{max} and h_{min} are not very sensitive to $V\left(h_{obs}\right)$ values close to 0 or 1. This is due to the diminishing sensitivity feature of PT captured by the usefulness value function curve. We have confirmed the same using sensitivity analysis. For most of the combinations of λ and α, the difference between h_{max} at $V\left(h_{obs}\right)$ = 0.001 and h_{max} at $V\left(h_{obs}\right)$ = 0.0001 is not more than 1.5 s. Similar results are obtained when computing h_{min} for all values of $V\left(h_{obs}\right)$ in the range $0.99 \leq V\left(h_{obs}\right) \leq 0.997$ (note that $V\left(h_{obs}\right) > 997$ results in unrealistic h_{min}).

3.2.3 Weighting functions

We assume that each driver has a subjective headway range corresponding to each compliance level. The magnitude of the weight at a particular compliance level is governed by the probability of the observed headway falling in the headway range of that level, e.g., if the observed headway is very small, then the probability of this headway falling in the headway range of high compliance level will be very high, and the probability of this headway falling in the headway range of low compliance level will be very low. Accordingly, for this headway, the weight will be high at the high compliance level and low at the low compliance level. The weighting functions for low and high levels of driver compliance are formulated in such a way that they capture the headway weighting behaviour. Furthermore, the functions capture the PT trait of probability weighting i.e., small probabilities are weighted higher and large probabilities are weighted lower.

The low compliance weighting function
The low compliance weighting function ($W^{LC}(P_{LC})$) and the probability that an observed headway falls in a driver's low compliance range (P_{LC}) are given by Equations (6) and (7), respectively:

$$W^{LC}(P_{LC}) = \frac{P_{LC}{}^{\gamma}}{(P_{LC}{}^{\gamma} + (1 - P_{LC})^{\gamma})^{1/\gamma}} \tag{6}$$

$$P_{LC} = \min\left(\frac{h_{obs}}{h_{max}}, 1\right) \tag{7}$$

where γ is the shape parameter. The $W^{LC}(P_{LC})$ formulation is the same as PT weighting function. From Equations (6) and (7), as h_{obs} increases and approaches to h_{max}, the low compliance weight increases and approaches to 1. Figure 5 depicts the same relationship.
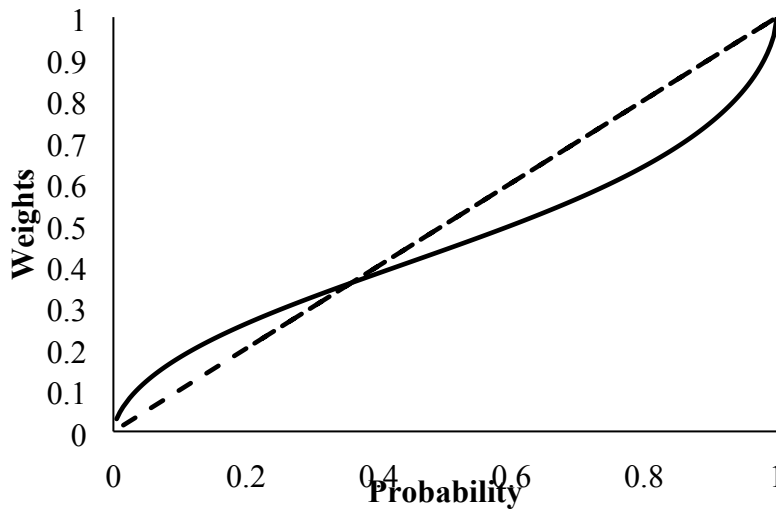

Figure 5 Plots of the weighting functions (Solid curve: Low compliance/High compliance weighting behaviour at $\gamma = 0.55$; Dashed line: linear weighting behaviour).

The high compliance weighting function

13

The high compliance weighting function ($W^{HC}(P_{HC})$) and the probability that an observed headway falls in a driver's high compliance range (P_{HC}) are given by Equations (8) and (9), respectively:

$$W^{HC}(P_{HC}) = \frac{P_{HC}{}^{\gamma}}{\left(P_{HC}{}^{\gamma} + (1 - P_{HC})^{\gamma}\right)^{1/\gamma}} \tag{8}$$

$$P_{HC} = \min\left(\frac{h_{min}}{h_{obs}}, 1\right) \tag{9}$$

where γ is the shape parameter. A different shape parameter is not required because both the compliance levels represent gains (driver is following the information), though different in magnitude. From Equations (8) and (9), as h_{obs} decreases and approaches to h_{min}, the high compliance weight increases and approaches to 1. Figure 5 depicts the same relationship.

3.2.4 Formulating compliance utilities

Because only a single value of observed headway is possible at the time of information display, the usefulness value is the same across both levels of compliance. However, drivers can weigh the information differently at different levels of compliance; accordingly, two weights are used to compute the compliance utilities for the two levels of compliance (one weight for one level). Hence, we formulate the simple prospects for low compliance and high compliance as (h_{obs}, P_{LC}) and (h_{obs}, P_{HC}), respectively. Equations (10) and (11) show the compliance utility formulations for low compliance and high compliance, respectively, and Equation (12) shows the maximum utility formulation:

$$UT^{LC}(h_{obs}, P_{LC}) = V\left(h_{obs}\right) W^{LC}(P_{LC}) \tag{10}$$

$$UT^{HC}(h_{obs}, P_{HC}) = V\left(h_{obs}\right) W^{HC}(P_{HC}) \tag{11}$$

$$UT = \max\left(UT^{LC}, UT^{HC}\right) \tag{12}$$

where UT^{LC} and UT^{HC} are compliance utilities of low and high compliance levels, respectively. The usefulness value associated with the observed headway is $V\left(h_{obs}\right)$, same at both the levels as explained above. The probabilities that an observed headway will fall under low and high compliance headway ranges are P_{LC} and P_{HC}, respectively, and the corresponding weights are $W^{LC}(P_{LC})$ and $W^{HC}(P_{HC})$. The maximum utility is denoted by UT that ranges from 0 to 1, with $UT = 0$ representing no compliance and $UT = 1$ representing the full compliance. The result from Equation (12) depicts the compliance level chosen by the driver. Note that the probabilities P_{LC} and P_{HC} belong to two different i.e., P_{LC} belongs to low compliance prospect and P_{HC} belongs to high compliance prospect, therefore, they are independent to each other and their sum can be greater or smaller than 1. Furthermore, as mentioned in Section 3.2.3, low compliance and high compliance headway ranges are subjective, thus, the probabilities associated with these ranges are latent and cannot be measured directly. More specifically, P_{LC} and P_{HC} represent surrogate measures of low compliance and high compliance latent probabilities and as P_{LC} and P_{HC} increase, the associated latent probabilities also increase e.g.,

if the observed headway is small, then P_{HC} will be high and thereby the high compliance probability will be high.

The complete process of a driver compliance decision making based on PT is summarised in the first block of Figure 6, and a hypothetical case is presented in the second block of Figure 6. The driver receives a warning message 'leader braking hard' at a headway of 2 seconds, he/she goes through the decision-making process as depicted in this figure, and eventually decides to comply high, i.e., high deceleration, because the high compliance prospect gives the maximum utility in this particular example.

More specifically, the driver compliance decisions are evaluated for six observed headways (1 to 10 sec) to showcase the efficacy of PT based modelling of driver compliance decision process. The results are reported in Table 2 where, as the observed headway increases, the usefulness value associated with the information decreases, thereby the maximum utility value decreases. Moreover, for each observed headway different weights to the same information at different levels of compliance can be observed. Table 2 also demonstrates how high or low compliance weights vary against observed headways. As the headway increases, the high compliance weight decreases while the low compliance weight increases. The table highlights the importance of both the usefulness value function and weighting function in evaluating compliance utility values and the level of compliance. The evidences from Figure 6 and Table 2 corroborate that PT based modelling of driver compliance decision process is realistic and behaviourally sound.
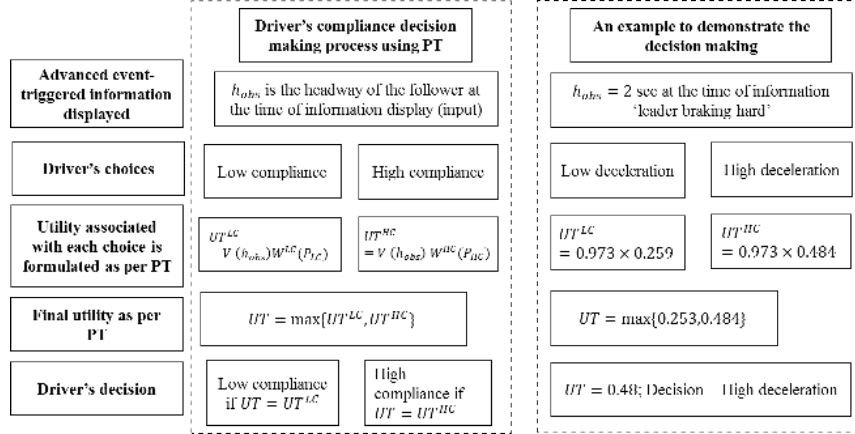
Figure 6 An example: a driver compliance decision-making process modelled using PT ($\lambda = 6, \alpha = 0.2, and \gamma = 0.65$).

Table 2 Driver compliance final utility calculation for six observed headways ($\lambda = 6, \alpha = 0.2 \ and \ \gamma = 0.65$).

h_{obs}	$V(h_{obs})$	$W^{LC}(P_{LC})$	$W^{HC}(P_{HC})$	UT^{LC}	UT^{HC}	$UT(h_{obs})$
1	0.992	0.178	1.000	0.177	0.992	0.992
2	0.973	0.259	0.497	0.253	0.484	0.484

4	0.768	0.382	0.324	0.293	0.251	0.293
6	0.231	0.497	0.259	0.115	0.060	0.115
8	0.026	0.640	0.222	0.017	0.005	0.017
10	0.002	1.000	0.197	0.002	0.000	0.002

4. CONNECTED VEHICLE DRIVING STRATEGY (CVDS)

This section presents the proposed CVDS that can be integrated with traditional CF models. CVDS has two parts: the first part (section 4.1) modifies the traditional CF models to model the driver's response to continuous information, and the second part (section 4.2) models the driver's behaviour in response to advanced event-triggered information. Importantly, the driver compliance is an integral component of both the parts.

4.1 CVDS Part I: Modelling the driver's response to continuous information

A comparison of microscopic traffic flow parameters (e.g., average headway, average spacing, average speed, fluctuations in speed and spacing, etc.) between the baseline and connected scenarios revealed that headway increases, and acceleration behaviour becomes more stable in the connected scenario (see Section 6.3). The time gap and headway are directly proportional to each other, and the recent literature suggests that when the desired time gap increases, the stability of CF models like IDM increases (Sun et al., 2018). Thus, the time gap parameter in CF models is multiplied with $(1 + UT(h_{obs}))$ to accommodate the impact of driver compliance with continuous information.

4.2 CVDS Part II: Modelling the driver's response to advanced event-triggered information

In response to the warning message 'leader braking hard', the driver decelerates to achieve a desired headway (h_{des}) from his/her reference headway (h_{obs}). The desired headway is the headway a driver desires to maintain when he/she is aware of an immediate emergency situation. In addition, the driver responses in τ seconds after the advanced message is displayed. Here, τ represents the delay in the driver's response to the advanced message. Note that the response delay τ is utilised while calibrating the integrated CF model. The required deceleration rate, d_n is provided in Equation (13):

$$d_n = -D \times \left(\frac{t_c}{T_c}\right)^n \tag{13}$$

where t_c varies from 0 to T_c with $t_c = 0$ at the start of deceleration process and $t_c = T_c$ at the end of the deceleration process, T_c is the response period, i.e., the time taken by the driver to attain D, and it depends upon the aggressiveness of the driver, and n is the time factor $\left(\frac{t_c}{T_c}\right)$ exponent and is equal to 3 for this study. Fixing the value of n was a deliberate decision in order to better facilitate the calibration of more important driver behaviour parameters. To fix the parameter, we performed simulations and found that a cubic deceleration rate is closer to

the observations. At $t_c = T_c$, the maximum deceleration D is reached, as given in Equation (14):

$$D = min\left\{b_{max}, (1 + UT(h_{obs})) \times \frac{b_{max} \times (1 - \frac{h_{obs}}{h_{des}})}{required\ deceleration}\right\} \qquad (14)$$

where b_{max} is the maximum allowable deceleration, and $UT(h_{obs})$ is the utility value calculated at h_{obs}. Note that contrary to the desired deceleration (b) parameter in IDM, b_{max} is the maximum physically possible value of deceleration that is limited by the car's braking capability. The parameter b_{max} is relatively a new parameter in traffic flow modelling. Therefore, we measured the variable from the data collected from the simulator experiment and the average value of b_{max} for 78 participants at emergency is 8.16 m/s². Thus, in calibration, we have fixed b_{max} equal to 8 m/s². The factor $(1 - \frac{h_{obs}}{h_{des}})$ is multiplied with b_{max} to account for high/low deceleration when the difference between h_{obs} and h_{des} is large/small. The required deceleration is multiplied by a factor equal to $(1 + UT(h_{obs}))$ that incorporates the impact of the compliance on the deceleration. Next, h_{obs} is measured at the time when the advanced message is received by the follower. It is reasonable to assume that the data from the follower (a connected vehicle) will have the information about when messages are received by the driver, and using such information one can measure h_{obs} corresponding to a specific message, in this case, the advanced message.

Note that CVDS part II is applicable only when $h_{des} > h_{obs}$, otherwise CVDS part I is used for modelling driver's response to the advanced event-triggered information as well. In addition, the parameter h_{des} is more likely to vary across different situations and human factors. However, to control the complexity of the model and similar to how researchers often treat other similar parameters (e.g., desired speed, desired deceleration, and etc.), it is reasonable to assume h_{des} (a model parameter) remains constant for a driver. Furthermore, the condition $h_{des} > h_{obs}$ does not guide the calculation of $UT(h_{obs})$; instead, it governs the acceleration or deceleration adopted when the advanced message is displayed. When simulating a CF model integrated with CVDS, $UT(h_{obs})$ is calculated first, and then the acceleration or deceleration is calculated. As mentioned above, $(1 + UT(h_{obs}))$ captures the driver compliance to messages in both CVDS parts I and II. It is calculated at each time interval for continuous information and also at the time when the advanced message is displayed. When the advanced message is displayed, the amplification effect i.e., $(1 + UT(h_{obs}))$ is the same in parts I and II because we are capturing driver compliance to the same message ('leader braking hard') in both cases and the magnitude will only depend on the h_{obs}. It will be unreasonable to use two different amplification effects in parts I and II because it implies that the driver is responding to two different messages which is obviously not the case here.

4.3 Integrating CVDS with IDM

For the purpose of demonstration, we select IDM and integrate it into CVDS. IDM belongs to the category of desired measures models (Saifuzzaman and Zheng, 2014), and assumes that the acceleration is a continuous function of the driver's speed, spacing to the leader, and speed difference between the leader and the follower. Equations (15) and (16) present the mathematical formulation of the IDM acceleration function of the nth driver.

$$a_n(S_n, V_n, \Delta V_n) = a \left[1 - \left(\frac{V_n}{V_0} \right)^{\delta} - \left(\frac{s^*(V_n, \Delta V_n)}{S_n} \right)^2 \right] \tag{15}$$

$$s^*(V_n, \Delta V_n) = s_0 + TV_n + \frac{V_n \Delta V_n}{2\sqrt{ab}} \tag{16}$$

where V_0, δ, T, s_0, a, and b are desired speed (m/s), free acceleration exponent, desired time gap (s), standstill distance (m), maximum acceleration (m/s^2), and desired deceleration (m/s^2), respectively. Moreover, a_n is the IDM acceleration (m/s^2), s^* is the desired spacing (m), V_n is the speed (m/s), ΔV_n is the relative speed (m/s) (difference of the follower's speed V_n and the leader's speed V_{n-1}), and S_n is the distance gap (m).

Corresponding to the two parts of CVDS discussed above, the integrated CVDS-IDM also has two parts, as shown in Figure 7. Part I is similar to the original IDM except that it has a modified time-gap parameter; and Part II is for modelling the driver's response to advanced event-triggered information, and has the same functional form as mentioned in Section 4.2.

While implementing CVDS-IDM, the switching between Part I and Part II might cause an abrupt jump in a very short period, which can be avoided by applying a smoothing function. Many smoothing functions can be used, while in this study, moving average smoothing is adopted to keep the smoothing step simple.
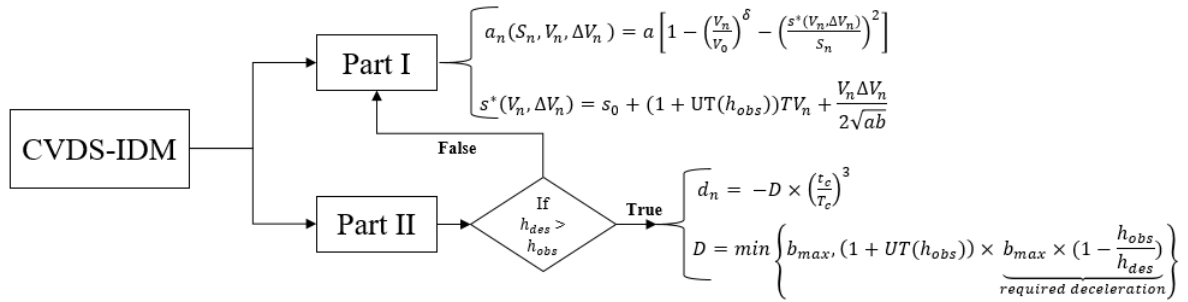

Figure 7 Schematic of integrated CVDS-IDM.

5. Calibration Methodology

The CVDS-IDM model is calibrated using the CV trajectory data collected from the driving simulator experiment. CF model calibration is essentially an optimization problem that involves minimizing the difference between the observed follower and the simulated follower, and finding the optimal model parameters. The simulated follower is generated using the CF model under consideration and its parameters are sampled from their predefined ranges. The

deviation of the simulated follower from the observed follower is expressed as an error using goodness-of-fit (GoF) functions and the CF feature (variable in GoF) which is compared between the two trajectories is called as a measure of performance (MoP). A combination of MoP and GoF is termed as an objective function, which is minimized using an optimization algorithm (OA). For a review of current studies on CF model calibration issues, refer to Sharma et al. (2018b).

5.1 Selection of a calibration setting

The uncertainty involved in the calibration process due to the elements above (particularly OA) affects the accuracy and the reliability of the calibration results. Thus, the calibration setting (i.e., a combination of MoP, GoF, and OA) is often evaluated for its efficacy before calibrating a CF model (Punzo et al., 2015, 2012; Saifuzzaman et al., 2015; Sharma et al., 2018b). The evaluation process involves examining different calibration settings using synthetic data (data generated by the model itself) followed by choosing the one that results in the lowest calibration errors. For CVDS-IDM, we have rigorously tested the suitability of an effective calibration setting, i.e., spacing as MoP (Ossen and Hoogendoorn, 2008; Punzo et al., 2012; Punzo and Montanino, 2016; Ranjitkar et al., 2004; Treiber and Kesting, 2013a), root mean square normalised error (RMSNE) as GoF (Ciuffo and Punzo, 2010; Punzo and Simonelli, 2005; Sharma et al., 2018b), and genetic algorithm (GA) as OA (Kesting and Treiber, 2008; Monteil et al., 2014; Punzo et al., 2012; Ranjitkar et al., 2004). The mathematical formulation of RMSNE with spacing as MoP is shown in Equation (17):

$$RMSNE = \sqrt{\frac{1}{N}\sum_{i=1}^{N}\left(\frac{S_i^{act} - S_i^{sim}}{S_i^{act}}\right)^2} \tag{17}$$

where RMSNE with spacing as MoP denotes the objective function, S_i^{act} denotes the actual value of spacing at i^{th} time step, S_i^{sim} denotes the simulated spacing at i^{th} time step, and N denotes the total time steps.

While testing the calibration setting, GA parameters are set as follows: the population size is 200, the maximum number of generations is 600, the maximum number of stall generations is 50, and the function tolerance is 1e-6. Furthermore, the upper and the lower bounds for CVDS-IDM parameters are set for improving the computational tractability of GA based optimization process. These parameters are detailed in Table 3.

When calibrating the CF model using GA, each optimization run (iteration) and different optimization start points results in slightly different solution because of two reasons: a) GA based search process is stochastic; and b) a plateau without a distinctive global minimum is present in the objective function surface (Punzo et al., 2012; Sharma et al., 2018b). Therefore, the calibration process is repeated 10 times with five different starting points. Furthermore, the calibration error (or fitting error) is calculated at each optimization run to quantify the performance of calibration setting. The calibration error is the minimum value of objective function obtained at the end of the optimization process and given by Equation (18):

$$\text{Calibration Error} = \min(RMSNE) \times 100 \tag{18}$$

Note that the calibration error reflects the fitting capability of any CF model (a lower calibration error indicates a better fitting capability). The final calibrated parameters set is the one with the minimum calibration error among all the 50 errors (5 starting points $\times$ 10 runs with each starting point).

Table 3 CVDS-IDM parameter bounds given as input in optimization.

Parameter	Lower Bound	Upper Bound
Desired speed $(V_0)(m/s)$	1	40
Acceleration exponent (δ)	0.1	5
Desired time gap (T) (s)	0.1	4
Standstill distance (s_0) (m)	1	10
Maximum acceleration $(a)(m/s^2)$	0.1	4
Desired deceleration $(b)(m/s^2)$	0.1	4.5
Response delay $(\tau)(s)$	0.1	3
alpha (α)	0.1	0.5
Gamma (γ)	0.5	1
lambda (λ)	5	10
Maximum possible deceleration (b_{max}) (m/s^2)	8	
Desired headway (h_{des}) (s)	1	5
Response period (T_c) (s)	1	5

Testing of the calibration setting requires a synthetic follower. To generate the synthetic follower, first, a leader's trajectory is randomly selected from the trajectory pairs obtained from the driving simulator experiment. The synthetic follower is generated using CVDS-IDM with parameters $V_0 = 30.6 \, m/s$, $\delta = 4$, $T = 2.1$ s, $s_0 = 10 \, m$, $a = 1.79 \, m/s^2$, $b = 2.69 \, m/s^2$, $\tau = 0.2 \, s$, $\alpha = 0.35$, $\gamma = 0.6$, $\lambda = 9.8$, $b_{max} = 8 \, m/s^2$, $h_{des} = 4.5 \, s$, and $T_c = 4.9 \, s$. Using the selected calibration setting, CVDS-IDM calibration is performed and calibration errors are calculated. Table 4 reports the synthetic data calibration results (arranged in decreasing order of the calibration error). Since it is difficult to show all the 50 calibration errors with corresponding model parameters, in Table 4 we only show the calibration error which is the minimum error among 10 runs for a particular starting point, and the corresponding calibrated parameter set. The parameters obtained from the 3rd start point leads to the minimum calibration error i.e. 0.371 %, and hence it is the final calibrated parameter set. The difference between the final parameter set and the actual parameters (ground truth) used for generating the synthetic follower is very small. Therefore, the adopted calibration setting works efficiently as expected. Similar results are obtained for other leader-follower pairs.

Table 4 Calibration results with different start points.

Start point	V_0	δ	T	s_0	a	b	τ	α	γ	λ	h_{des}	T_c	Calibration error
1	29.5	4.9	2.0	9.8	1.7	2.0	0.4	0.3	0.9	9.9	2.8	1.7	0.29 %
2	34.8	2.5	1.9	10	1.8	1.9	0.1	0.3	1	6.7	1.5	4.9	0.28 %
3	**31.4**	**4.0**	**2.1**	**9.7**	**1.7**	**2.0**	**0.2**	**0.3**	**0.5**	**5.0**	**4.5**	**4.8**	**0.26 %**
4	36.8	2.6	1.5	9.9	1.7	1.1	0.6	0.2	1	5.0	3.8	4.4	0.28 %
5	29.8	4.9	2.0	9.6	1.7	2.0	0.2	0.3	0.8	9.6	2.9	4.8	0.29 %

5.2 Calibration process for CVDS-IDM

CVs will not only provide high-resolution trajectory data but also the time information regarding when the vehicles receive the messages. Based on these benefits, a calibration methodology is framed particularly for CVs and described in Table 5. CVDS-IDM is a single model with two parts and when calibrating CVDS-IDM the entire trajectory is utilised in the same way as when we calibrate other CF models in general. Meanwhile, the original IDM is calibrated using the trajectory pairs in the baseline scenario to understand the impact of CE on CF behaviour by comparing the common parameters between CVDS-IDM and IDM.

Table 5 Methodology for calibrating IDM and CVDS-IDM.

Scenario	Time frame	Model calibrated	Equation	Remark
Baseline	t_{start} to t_{end}	IDM	Equations (15) and (16)	t_{start} and t_{end} are the start and the end time of the trajectory
Connected	t_{start} to $(t_1 - \Delta t)$	CVDS-IDM (Part I)	Figure 7	$t_1 = t_m + \tau$, where t_m is the time when the advanced warning message is displayed and τ is the response delay. $UT(h_{obs})$ is calculated at each time instant and Δt is the time step.
	t_1 to t_2	CVDS-IDM (Part II)	Figure 7	$t_2 = t_1 + T_c$. Whenever the advanced warning message appears, the acceleration will be governed by either CVDS-IDM Part I or II depending upon whether the condition $h_{des} > h_{obs}$ is true or not.
	$(t_2 + \Delta t)$ to t_{end}	CVDS-IDM (Part I)	Figure 7	

6. Results and Discussion

6.1 Calibration results and findings

The IDM and CVDS-IDM models are calibrated using 78 trajectory pairs in the baseline and connected scenarios, respectively, and employing the selected calibration setting discussed above. Figures 8 and 9 depict the frequency distributions of calibrated parameters of both models. Figure 10 presents the respective calibration errors.

The distributions of calibrated parameters (Figures 8 and 9) attribute to the existence of inter-driver heterogeneity (i.e., driving style variability among the participants), while the average values reflect the average driving behaviour of the 78 participants. The average fitting errors are 17.3 % and 13.3 % for IDM and CVDS-IDM models, respectively (Figure 10).

The errors are consistent with the typical error ranges reported in previous studies, i.e., 15% to 25% (Brockfeld et al., 2004; Kesting and Treiber, 2008; Punzo and Simonelli, 2005; Sharma et al., 2018b). Overall, calibration results show that both IDM and CVDS-IDM are capable of describing local CF dynamics in the baseline and connected scenarios, respectively.
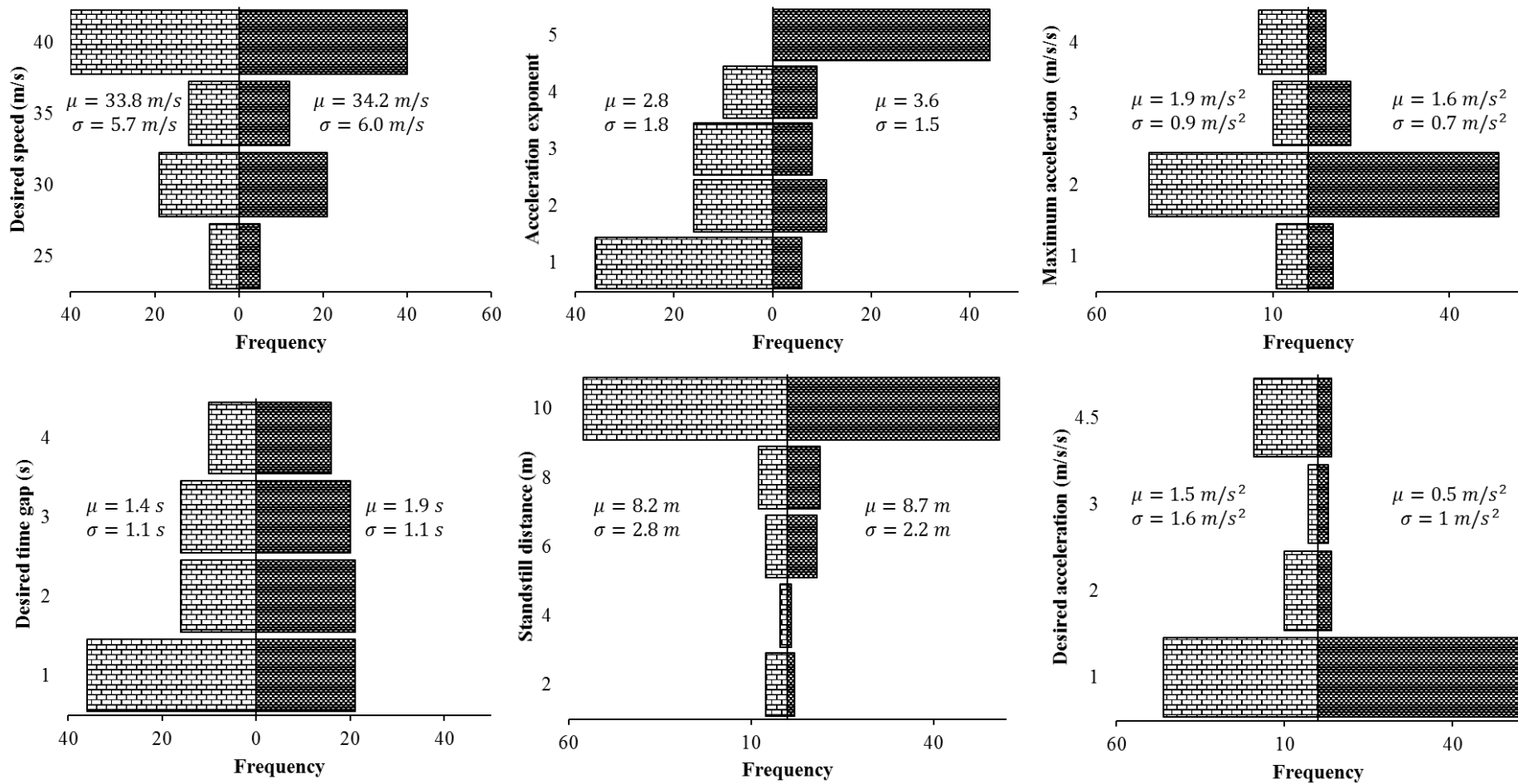
Figure 8 Distributions of the calibrated parameter values common in CVDS-IDM (Connected) and IDM (Baseline). In each plot, μ and σ represent the mean and the standard deviation of calibrated parameters, respectively.
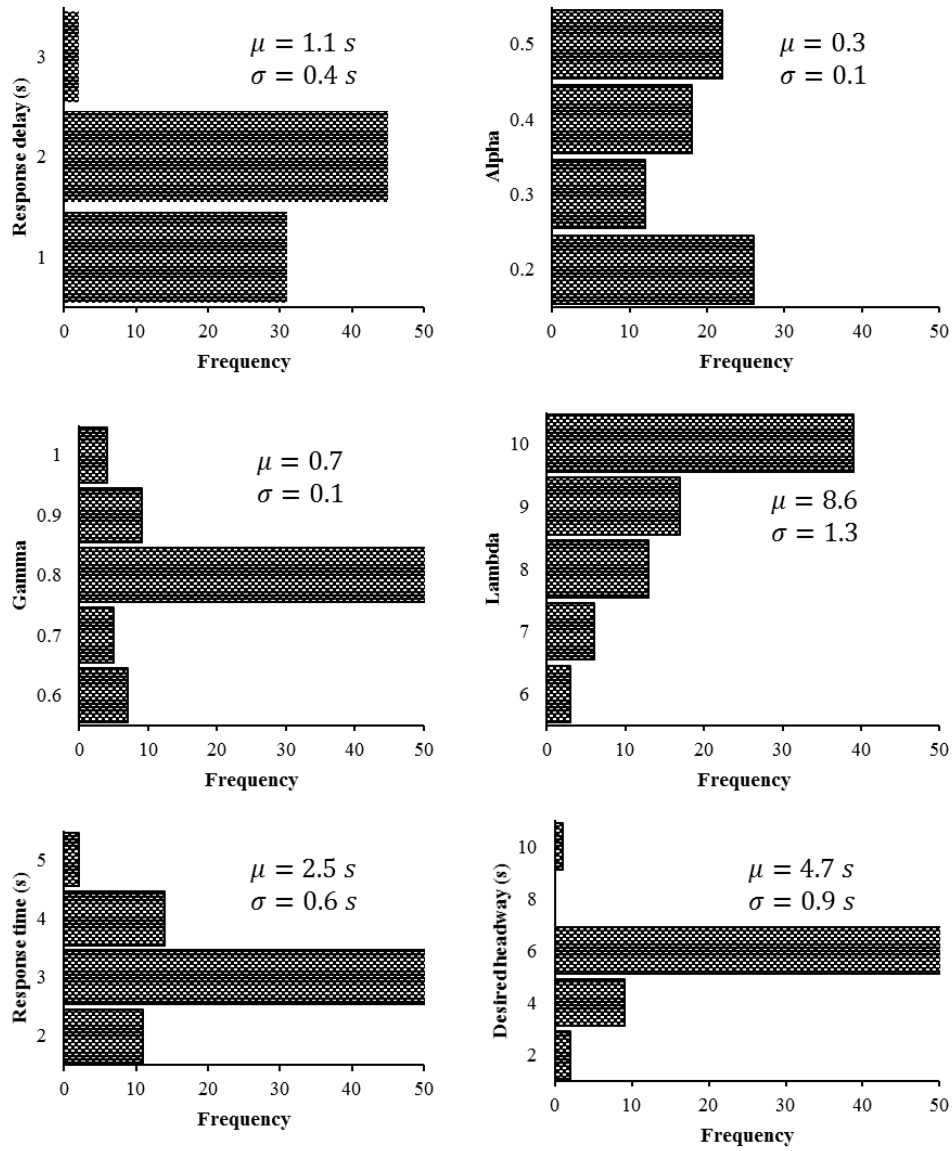
Baseline   Connected

Figure 10 Distributions of the remaining CVDS-IDM calibrated parameter values. In each plot, μ and σ represent the mean and the standard deviation of calibrated parameters, respectively.
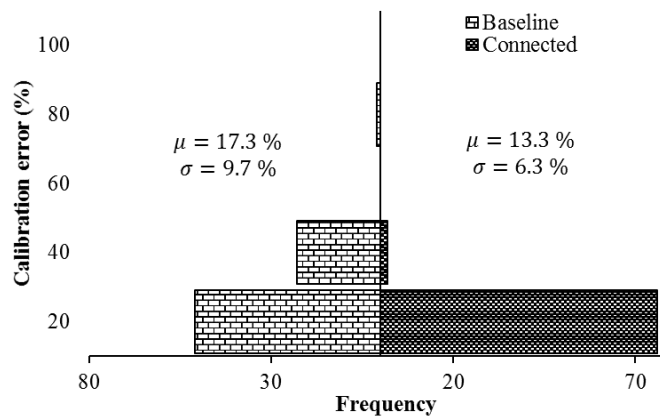

Figure 9 Distribution of the calibration errors for CVDS-IDM (Connected) and IDM (Baseline).

A two-sample t-test is performed between the common parameters of IDM and CVDS-IDM to understand the changes in driving behaviour ascribed by the CE (Figure 8). Among the six common parameters, acceleration exponent (δ) (*p-value* = 0.001), desired time gap (T) (*p-value* = 0.02), and maximum acceleration (a) (*p-value* = 0.006) are found to be statistically different at a 5% significance level. These findings provide insights into the changes in driving behaviour, as elaborated below. Based on CVDS-IDM's mathematical formulation, the acceleration exponent (δ) governs the reduction in the acceleration as the vehicle's speed approaches the desired speed.

A larger acceleration exponent (δ) means a more gradual reduction in acceleration. Meanwhile, the safety distance with the leading vehicle is given by the formula $s_0 + vT$. Hence, an increase (decrease) in the desired time gap (T) leads to an increase (decrease) in the safety distance with the leader. In the connected scenario, the acceleration exponent (δ) and the desired time gap (T) are larger, but the maximum acceleration (a) is smaller compared to the values in the baseline scenario. These results signify that in the CE, drivers accelerate more cautiously, decelerate more gradually when approaching the desired speed, and maintain a larger safety distance with the leader. Overall, we can label such driving behaviour in the CE as 'conscientious driving behaviour'. Talking about the combined effect, a larger δ results in a larger acceleration and a larger T results in a lower acceleration, thereby countering each other. However, from the mathematical formulation of IDM or CVDS-IDM for that matter, the change in T and a will overpower the change in δ. We have confirmed this conclusion using simulations as well.

The parameters response delay (τ), desired headway (h_{des}), and response period (T_c) govern the driver's response to the advanced information about an emergency. Based on the calibration results (Figure 9), in response to the advanced warning of the leader's hard braking, on average the participants maintain a desired headway of 4.7 s, respond to the advanced information in 1.1 s, and attain the deceleration required to achieve the desired headway in 2.5 s. An aggressive/conservative driver compared to the average driver is characterised by a lower/higher response delay, desired headway, and response period.PT parameters alpha (α), lambda (λ), and gamma (γ) govern the shapes of usefulness value and weighting function curves whereby influencing the driver compliance behaviour. Figure 11 displays the usefulness value and the weighting function curves for the average PT parameters (average of the calibrated PT parameters), and for the parameters greater and smaller than the average. Note that the average PT parameters describe an averaged compliance behaviour. Figure 11 assists in understanding the difference between the compliance behaviour of a driver and the average compliance behaviour.
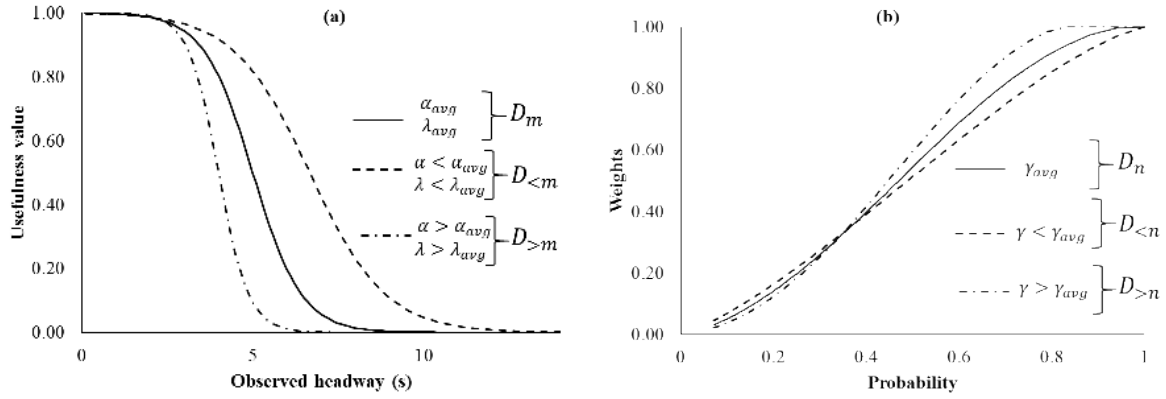
Figure 11 Effect of different PT parameters on the usefulness value function curve ((a)) and high-compliance weighting function curves (b)).

Figure 11 (a) shows the usefulness value function curves. To facilitate our discussion, three groups of drivers are defined: $D_{>m}$ is the group of drivers with PT parameters $[\alpha,\lambda] > [\alpha_{avg},\lambda_{avg}]$, D_m is the group of drivers with PT parameters equal to $[\alpha_{avg},\lambda_{avg}]$, and $D_{<m}$ is the group of drivers with PT parameters $[\alpha,\lambda] < [\alpha_{avg},\lambda_{avg}]$. $D_{>m}$ is more sensitive to a change in the observed headway than D_m as indicated by the steeper curve of $D_{>m}$. A small decrease (increase) in the observed headway can significantly increase (decrease) the usefulness value of an information in case of $D_{>m}$. Moreover, the usefulness region (i.e., the area under the usefulness value curve) of $D_{>m}$ is smaller than that of D_m, which implies that the information assistance is less useful (in terms of headway range and magnitude of usefulness) for $D_{>m}$. Meanwhile, $D_{<m}$ is less sensitive to a change in the observed headway and has a bigger usefulness region, which implies that the information assistance is more useful for $D_{<m}$.

Similarly, to facilitate our discussion on weighting function curves (Figure 11(b)), three groups of drivers are defined: $D_{>n}$ is the group of drivers with PT parameters $[\gamma] > [\gamma_{avg}]$, D_n is the group of drivers with PT parameters equal to $[\gamma_{avg}]$, and $D_{<n}$ is the group of drivers with PT parameters $[\gamma] < [\gamma_{avg}]$. For the same probability and information, $D_{>n}$ weighs the information higher than D_n, while $D_{<n}$ weighs the information lower than D_n. The degree of trust in the information assistance system is one of the factors for such variability in weighing the same information. Madsen and Gregor (2000) define human computer trust as "the extent to which a user is confident in, and willing to act on the basis of, the recommendations, actions, and decisions of an artificially intelligent decision aid." Accordingly, the three groups of drivers can be arranged in the decreasing order of trust in the information assistance: $D_{>n}$, D_n, and $D_{<n}$. Note that similar inferences can be drawn from the low-compliance weighting function curves.

6.2 CVCF behaviour modelling: Comparing the performance of CVDS-IDM and a traditional CF model

In previous studies, traditional CF models i.e., models developed for vehicles in traditional environment, are often used to describe CVCF behaviour. The behavioural accuracy of the traditional CF models in modelling CVCF behaviour is questionable or even problematic, primarily because these models are calibrated using trajectory data of traditional vehicles. Thus, the next natural step is to calibrate a traditional CF model using CV trajectory data and

compare it with CVDS-IDM. In this regard, the IDM is calibrated using the trajectories of connected scenario, and the numerical and the behavioural soundness of CVDS-IDM and IDM are compared. The purpose of comparing CVDS-IDM with IDM is not for discrediting IDM, but for illustrating the necessity of introducing CVDS to IDM, i.e., the necessity of introducing "the trigger", or the unsoundness of directly using IDM (or any other traditional CF models) for modelling CF behaviour in CE.

6.2.1 Behavioural soundness

Behavioural soundness in this study is defined as models' capability to capture the signatures of driving behaviour in a traffic environment in the present case CF behaviour in CE. This section explores whether CVDS-IDM and IDM are behaviourally sound or not. The observed speed profiles of the leader and the follower in the baseline and connected scenarios are displayed in Figures 12(a) and 12(b), respectively. In Figure 12(a), the follower reacts (decelerates) after the leader has started deceleration (stimulus-response behaviour) while in Figure 12(b), the follower reacts to the advanced event-triggered information ('Leader braking hard') and decelerates before the leader decelerates (proactive behaviour). Such proactive behaviour in the connected scenario is evident in both the high-speed as well as the low-speed regions. For the leader-follower pair under consideration, Figure 12(b) also depicts the simulated speed profiles generated using CVDS-IDM and IDM, respectively. The simulated speed profiles are generated after calibrating CVDS-IDM and IDM using connected scenario data. From Figure 12(b), CVDS-IDM reacts to the advanced information and decelerates before the leader decelerates, which is consistent with the observed behaviour of the follower. In contrast, IDM is unable to capture this proactive behaviour.

Furthermore, a paired t-test is performed between the observed response delays and the calibrated response delays (τ) to underscore the capability of CVDS-IDM in describing the CVCF behaviour. The observed response delays are calculated as the difference between the time when the message is delivered to the participant and the time when the participant starts pressing the brake pedal (accelerator and brake pedal pressure data are collected during the simulator experiment). The test reveals there is no statistical difference between the observed response delays and the calibrated response delays (*p-value* = 0.87) at 5% significance level. This further confirms the efficacy of CVDS in accurately reproducing the follower's proactive behaviour in the CE. Additionally, this highlights that CVDS parameters e.g., τ, are physically measurable.

Importantly, CVDS-IDM incorporates a driver compliance behaviour in the presence of the information assistance, which is a significant advantage over IDM. As mentioned before, driver compliance with the information will play a key role in the success of connected vehicle technologies.

6.2.2 Numerical soundness

Numerical soundness in our study is defined in terms of calibration errors. A model is numerically sound if the calibration errors are within the acceptable range i.e., 20-25% (Brockfeld et al., 2004; Kesting and Treiber, 2008; Punzo and Simonelli, 2005; Sharma et al., 2018b). Note that in the literature a small calibration error is sometimes used as an evidence of

a model's behavioural soundness, on which we disagree since a calibration error, no matter how small, is essentially a numerical number that can be obtained from an arbitrary model.
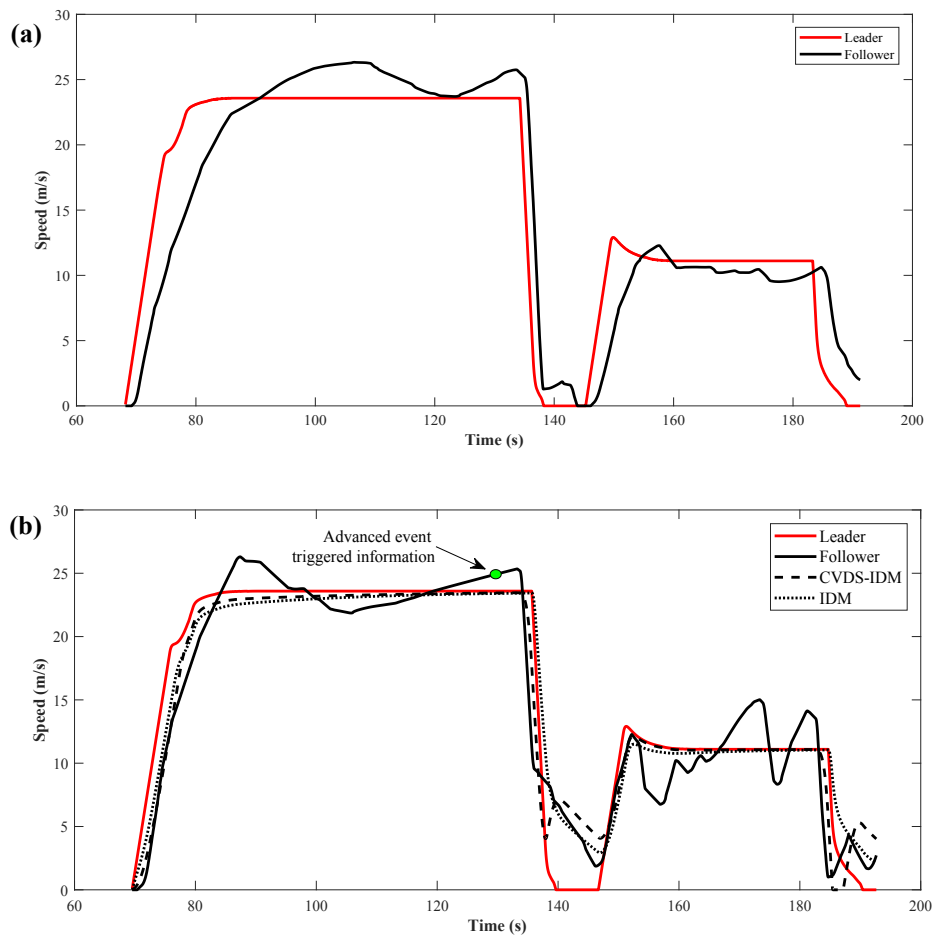

Figure 12 (a) Leader-follower speed profiles in the baseline scenario; (b) Leader, follower, CVDS-IDM follower, and IDM follower speed profiles in the connected scenario.

This section compares the numerical soundness of CVDS-IDM and IDM. In addition, we have also compared the calibrated parameter estimates of CVDS-IDM and IDM. Figure 13 displays the cumulative probability plots of the calibration errors for CVDS-IDM and IDM. Note that the plots are based on the calibration errors corresponding to all the 78 trajectory pairs. These plots clearly show the supremacy of CVDS-IDM over IDM. The 50th percentile values of the calibration errors for CVDS-IDM and IDM are 9.5% and 14.5%, respectively. In addition, 90% of the calibration errors for CVDS-IDM and IDM are below 18% and 25%, respectively. Moreover, the paired t-test results reveal statistically significant differences (p-value<0.05) between the two calibration error sets at 5% significance level. Therefore, the fitting capability of CVDS-IDM is significantly better than that of IDM.

Figure 14 illustrates a comparison of cumulative probability plots of calibrated parameters that are common in CVDS-IDM and IDM (except acceleration exponent). The desired speed (V_0) plot depicts that CVDS-IDM captures a good spectrum of desired speed values, which is highly likely considering the presence of inter-driver heterogeneity, while in case of IDM, more than 65% of the desired speed values are 40 m/s (145 km/h). Next, for IDM, 90% of the desired

28

deceleration values are below 0.7 m/s², which is significantly lower than the comfortable deceleration of 1.5 m/s² (Treiber and Kesting, 2013b). Similar observations can be observed for other parameters as well. Overall, the parameter estimates from CVDS-IDM more evenly spread than those from IDM, which indicates that inter-driver heterogeneity in the CE is better captured by CVDS-IDM.

In case of CF model calibration using real data trajectories, among several other important factors the calibration results depend on bound settings since they essentially govern the feasible region of the objective function within which the optimisation algorithm (iteratively) attempts to find the global minimum. Figure 14 shows that the calibrated parameters of IDM have skewed distributions as they are close to either the lower bound or the upper bound of the parameter range provided during the optimization process. Moreover, for CVDS-IDM, a few V_0 values are in the range of 20 m/s to 25 m/s i.e., close to the lower bound whereas for s_0 values are close to 10 m i.e., the upper bound. Furthermore, for IDM, around 65% of V_0 values are close to 40 m/s. Such calibrated parameters values have been observed previously, e.g., Kurtc and Treiber (2016) and Sharma et al. (2018b) obtained skewed distributions of parameter estimates when IDM was calibrated using NGSIM data (NGSIM, 2010). As reported in Sharma et al. (2018b), the optimisation algorithm often converges to local minima due to the presence of plateau (near the parameter bounds) in the surface plot of the objective function and hence, the calibrated parameter values are mostly close to the lower bounds or the upper bounds. For further details refer to Sharma et al. (2018b). As observed from Figure 14, CVDS-IDM parameters are less affected by such issue. Thus, CVDS-IDM can provide better parameter estimates.
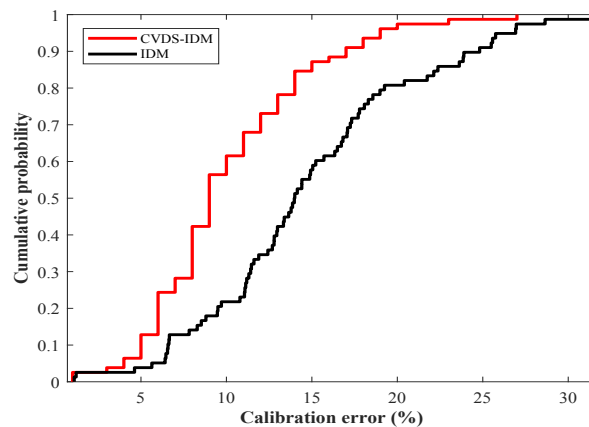

Figure 13 Comparison of the calibration errors between CVDS-IDM and IDM.

In addition to the issues in CF model calibration, there can be other contributing factors as well for such calibrated values. The driving simulator experiment setting can influence the driving behaviour because of its limited physical, perceptual, and behavioural fidelity. This in turn can affect the calibrated model parameters. Furthermore, driver heterogeneity that has been frequently reported and widely accepted in the literature (Ossen and Hoogendoorn, 2007, 2011) also impacts the CF model calibration results.

The results reported above unambiguously demonstrate that CVDS-IDM is more behaviourally and numerically sound than IDM in modelling CVCF behaviour. The results also reflect that

when human factors are carefully incorporated in traditional CF models, it can, not only assist in comprehensively describing the driving behaviour but also in obtaining reliable and realistic parameter estimates.
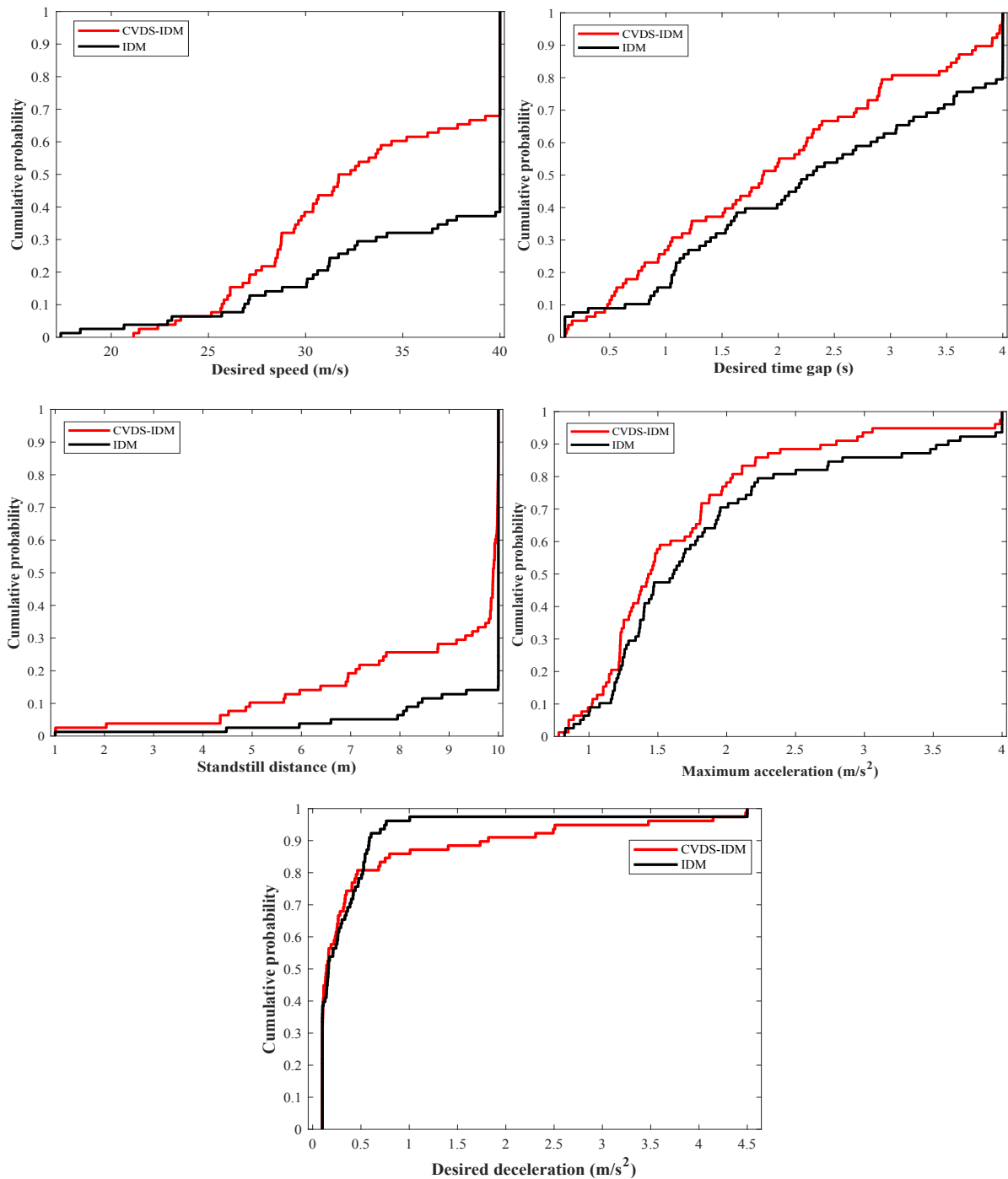

Figure 14 Comparison of calibrated parameters estimates between CVDS-IDM and IDM.

6.3 Understanding connected vehicle CF behaviour

Section 6.1 demonstrates the connected vehicle CF behaviour using the calibrated model parameters of CVDS-IDM. The previous section, using the driving simulator data, highlights a distinctive feature of CF behaviour in a CE environment i.e., how follower reacts to an advanced event-triggered message. This section reveals more insights about the connected

vehicle CF behaviour by comparing CF measures between the baseline and connected scenarios of the driving simulator experiment data of low speed section. A similar analysis can be carried out using high speed section as well. More specifically, four CF measures between the baseline and connected scenarios are compared namely, average spacing, average time headway, fluctuation in spacing, and fluctuation in speed. Average spacing is defined as the average of all the spacing values from the starting time to the end for a leader-follower pair. Average time headway is defined as the average of all the time headway values from the starting time to the end for a leader-follower pair. Fluctuation in spacing is calculated as the standard deviation of all the spacing values from the starting time to the end of for a leader-follower pair. Fluctuation in speed is defined as the standard deviation of all the speed values from the starting time to the end for a follower. Fluctuations in spacing and speed demonstrate how stable CF behaviour is in a given scenario.
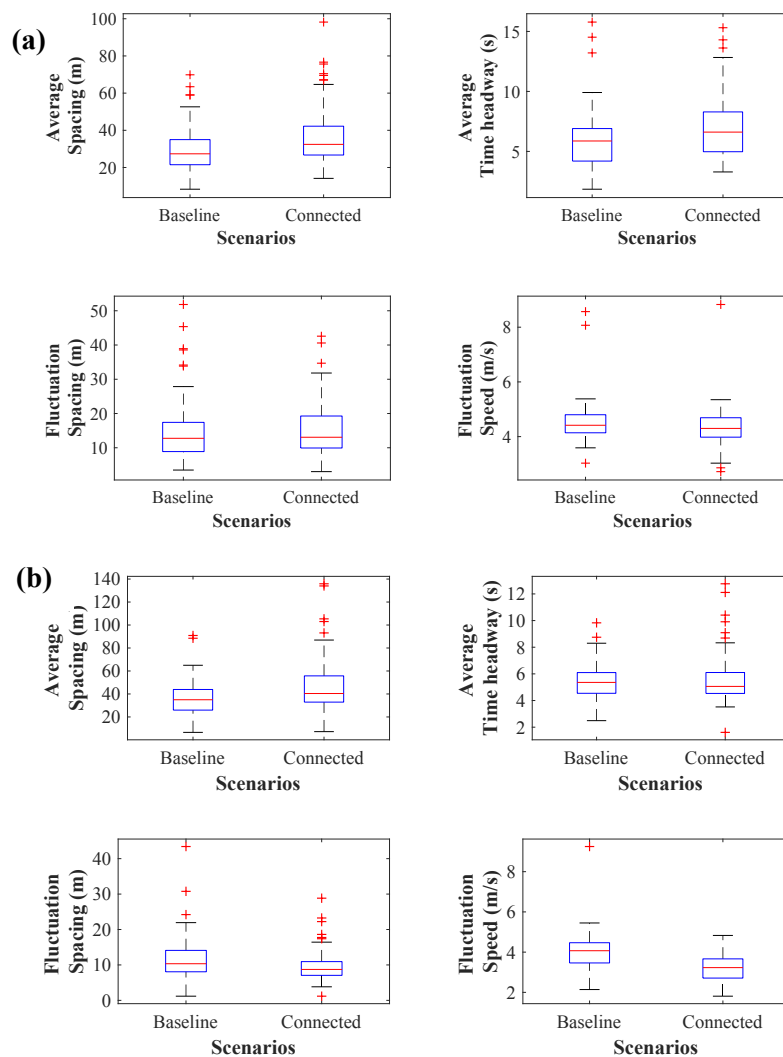

Figure 15 (a) Distributions of the CF measures of actual followers' behaviour in the baseline and connected scenarios; (b) Distributions of the CF measures of simulated followers' behaviour in the baseline and connected scenarios.

Note that our motive is to observe the relative change in a CF measure from the baseline to the connected scenario. Moreover, to further scrutinise the performance of CVDS-IDM these four CF measures are also calculated using simulated followers. These measures are then compared

and the consistency of relative change observed using simulated followers with the relative change observed using actual followers is examined. Actual followers are the followers in the simulator experiment. Each simulated follower in the baseline scenario is generated using IDM calibrated with baseline trajectories whereas each simulated follower in the connected scenario is generated using CVDS-IDM calibrated with traditional trajectories. The distributions of the CF measures in baseline and connected scenarios for the actual followers and for the simulated followers are shown in Figure 15. A paired t-test is carried out at the 90% level of significance to compare the means of CF measures in the two scenarios, and the results are reported in Table 7. Based on those CF measures that are statistically significantly different between baseline and connected scenarios, we can conclude that an actual follower maintains a larger headway, a larger time gap, and a small fluctuation in speed in the connected scenario. Fluctuation in spacing is not significantly different between these two scenarios, however, the mean fluctuation is smaller in the connected scenario. The findings demonstrate that in general CF behaviour in the connected scenario is safer as drivers maintain a larger safety margin (large spacing and time headway in connected scenario) and it is also more stable (low fluctuation in speed in the connected scenario) relative to CF behaviour in the baseline scenario. From Table 7, similar conclusions can be made using simulated follower results since average spacing, fluctuation in spacing, and fluctuation in speed are statistically significantly different (average time headway is not statistically significantly different, however, the mean average time headway is larger in the connected scenario). The results depict that CVDS-IDM CF behaviour is consistent with the actual CF behaviour in CE, thereby displaying CVDS-IDM's nice performance and behavioural soundness.

Table 6 Comparison of CF measures between baseline and connected scenarios for actual followers and simulated followers.

CF measure	Actual follower (Baseline vs Connected)		Simulated follower (Baseline vs Connected)	
	p-value	Inference	p-value	Inference
Average Spacing	0.004	Large in CE	<0.001	Large in CE
Average Time Headway	<0.001	Large in CE	0.491	-
Fluctuation in Spacing	0.973	-	<0.001	Small in CE
Fluctuation in Speed	0.074	Small in CE	<0.001	Small in CE

6.4 A note on the integrated CF model's complexity

CVDS has two parts: part I models the driver's response to continuous information about the leader's stimulus, and part II models the driver's response to advanced information about the leader's stimulus. The CVDS has 6 parameters (3 PT parameters and 3 additional parameters). The three PT parameters are alpha, lambda, and gamma. In case of modelling the driver's response to advanced information, 3 parameters are required and they are desired headway (

h_{des}), response delay (τ), and response period (T_c). Importantly, all 6 CVDS parameters are physically meaningful and behaviourally sensible. The 3 shape parameters of PT govern the essential traits of PT i.e., value and weighting functions (refer Section 3 for a detailed discussion). Section 4 provides the physical meanings of the remaining three parameters. CVDS parameters can be quantified using calibration as shown in Section 6.1 or using controlled experiments as shown in Section 6.2.2 (τ is measured using trajectories).

The final number of parameters will depend upon the CF model which is integrated with CVDS. When CVDS is integrated with IDM, there are 12 parameters in CVDS-IDM (6 IDM parameters and 6 CVDS parameters). We understand that calibrating these 12 parameters is not an easy task, and may lead to overfitting. Similar challenges exist for any other models, too. However, the critical point here is that we are trying to model CF behaviour with an additional component i.e., CE. That is, the physical system we are trying to approximate is distinctively different from and substantially more complex than the one traditional CF models aim to reproduce. Such extra complexity should be directly reflected in the extra complexity of a model, and it would be philosophically wrong if we assume that we could still be able to capture the CF behaviour in CE using a model with the same amount of complexity for capturing the CF behaviour in a TE (Wallace, 1996; Weisberg, 2013). Otherwise, the model's interpretability, explanatory capability, and predictive power would be inevitably compromised.

When developing a model for describing a more complex system, the focus should not be whether the model's complexity would increase or not (inherently it should increase), but whether each new parameter is behaviourally sound and convincingly justified. CVDS allows us to model connected vehicle CF behaviour comprehensively with physically meaningful and behaviourally sensible parameters. More specifically, it incorporates a critical and decisive human factor i.e., driver compliance, and models the impact of different kinds of information i.e., continuous and advanced. Hence, the advantages and benefits of CVDS far outweigh its computational disadvantages. Note that we have adopted a few measures to reduce model complexity e.g., fixing the values of parameters n and b_{max}, and T_c is treated as a model parameter rather than calculated as a function of speed, spacing and driver behaviour. Furthermore, when implementing this model, techniques like variance-based sensitivity analysis can be employed to reduce its computational complexity by revealing and fixing non-influential parameters of a CF model, as described in Punzo et al., (2015) and Sharma et al., (2018b).

7. Conclusions and future work

This paper presents a connected vehicle driving strategy (CVDS) which is capable of being integrated with CF models to comprehensively and realistically describe the car-following behaviour in a CE. The driver compliance—a key human factor for the success of connected vehicles (CV)—is an integral part of the CVDS. Moreover, the driver compliance is modelled using a widely accepted theory of decision making under risk – the Prospect Theory (PT). The value function and the weighting functions of PT are reformulated such that these functions are consistent with the driver compliance behaviour and with the key PT features. Using PT, the driver compliance behaviour has been formulated to have following features: a) as headway

decreases the driver compliance increases; and b) the driver's decision on whether and how much to comply with the information depends upon the observed headway.

To overcome the issue of unavailability of CV trajectory data, the CE was designed in an advanced driving simulator, and the driving simulator experiment was conducted with 78 participants.

CVDS is integrated with IDM (i.e., CVDS-IDM), and CVDS-IDM is calibrated using the data from the driving simulator experiment. The calibration results demonstrate that in CE, drivers accelerate more cautiously, decelerate more gradually when approaching the desired speed, and maintain a larger safety distance with the leader. Furthermore, follower maintains a larger headway, a larger time gap, and a small fluctuation in speed and spacing in the connected scenario. This shows when drivers are informed with surrounding traffic information they perform the CF task safely and efficiently in comparison to no information. In addition, CVDS-IDM is more behaviourally sound than IDM in modelling CVCF behaviour because it reacts to the advanced event-triggered information (consistent with the participants' behaviour observed in the experiment). Similarly, CVDS-IDM is more numerically sound because of low calibration errors and calibrated parameters estimates are more evenly spread. Since this research is based on driving simulator experiments, an important point to highlight here is that the results and the inferences made for CE using CVDS-IDM shall be comprehended relative to the traditional environment results rather than in the absolute terms.

It is important to highlight that results reported in the paper shall be looked through the relative lenses rather than the absolute since the study is based on driving simulator experiments. This signifies that although the results from this study demonstrate that CVDS-IDM model is capable of describing the CVCF behaviour, and is more behaviourally and numerically sound than IDM, the magnitudes of calibrated model parameters might not represent the true parameter values in the real world, and they are not directly transferable to the same or other real world CE scenarios. Hence, CVDS-IDM should be calibrated using the real world CE data to better gauge the model parameter ranges and distributions, and to improve the model's transferability. The current modelling framework i.e., CVDS focusses on the information from the leading vehicles only and thus, it can be extended to incorporate the effect of information from the lag vehicle. To this end, a dedicated study is required to understand what information from the lag-vehicle can be provided to drivers without increasing participants' workload. CVDS can be extended to model the CF behaviour in the presence of communication impairments (e.g., communication delay and communication loss), and to model the driver compliance behaviour while performing lane-changing manoeuvre (Zheng, 2014) in the CE. At present, the driver compliance is measured at each interval as per h_{obs} i.e., $UT(h_{\mathrm{obs}}(t))$. A straightforward way to incorporate the communication delay is to calculate UT with some time delay i.e., $UT(h_{\mathrm{obs}}(t + t_{\mathrm{d}}))$. This signifies that since information is delayed, the impact of driver compliance will also be delayed. Moreover, a straightforward way to incorporate communication loss is to set $UT(h_{\mathrm{obs}}(t)) = 0$, i.e., zero compliance because no information is provided.

The calibrated CVDS-IDM parameters hinted that driving behaviour in CE can be a 'conscientiousness driving behaviour.' Conscientiousness, one of the five factors in the Big Five Factor (BFF) model of personality (John and Srivastava, 1999), is a personality trait representing carefulness. A focussed study to explore whether the driving behaviour in CE is a 'conscientiousness driving behaviour' or not can be insightful. Furthermore, the calibrated values of PT parameters (i.e., α, λ, and γ) provide surrogate measures of a driver compliance and can assist in classifying drivers into different categories: low compliance, moderate compliance, and high compliance.

CVDS can also be used to investigate how the driver' compliance influences important traffic flow phenomena, e.g., stability (Sun et al., 2018), capacity drop (Chen et al., 2014), traffic hysteresis (Chen et al., 2012; Laval, 2011), and stop-and-go oscillations (Tian et al., 2015; Zheng et al., 2011a, 2011b). If we look at CVDS-IDM analytically, we have incorporated the impact of driver compliance as a stochastic desired time gap and a stochastic required deceleration. A comparison of CVDS-IDM with CF models having stochastic time headway term such as described in Tian et al. (2016) and Treiber et al. (2006) can be carried out after modifying these models to suit the CE. On similar lines, future research studies can focus on a comprehensive comparison of behavioural and numerical soundness of traditional CF models, modified traditional CF models (traditional CF models modified to be used in CE), and connected vehicle CF models in CE. Such work is ongoing.

Acknowledgements

References

Adell, E., Várhelyi, A., dalla Fontana, M., 2011. The effects of a driver assistance system for safe speed and safe distance–a real-life field study. Transp. Res. Part C Emerg. Technol. 19, 145–155.

Ali, Y., Zheng, Z., Haque, M.M., 2018. Connectivity's impact on mandatory lane-changing behaviour: Evidences from a driving simulator study. Transp. Res. Part C Emerg. Technol. 93, 292–309.

Attema, A.E., Brouwer, W.B.F., l'Haridon, O., 2013. Prospect theory in the health domain: A quantitative assessment. J. Health Econ. 32, 1057–1065.

Atzwanger, K., Ruso, B., 2004. Aspects of Humans Aggressive Driving Behaviour as Indicators for the Irrationality of Thinking, in: Human Behaviour and Traffic Networks. Springer, Berlin, Heidelberg, pp. 193–203.

Avineri, E., Bovy, P., 2008. Identification of Parameters for a Prospect Theory Model for Travel Choice Analysis. Transp. Res. Rec. J. Transp. Res. Board 2082, 141–147.

Avineri, E., Prashker, J., 2004. Violations of Expected Utility Theory in Route-Choice Stated Preferences: Certainty Effect and Inflation of Small Probabilities. Transp. Res. Rec. J. Transp. Res. Board 1894, 222–229.

Barberis, N., Huang, M., 2008. Stocks as Lotteries: The Implications of Probability Weighting for Security Prices. Am. Econ. Rev. 98, 2066–2100.

Ben-Yaacov, A., Maltz, M., Shinar, D., 2002. Effects of an in-vehicle collision avoidance warning system on short-and long-term driving performance. Hum. Factors J. Hum. Factors Ergon. Soc. 44, 335–342.

Brockfeld, E., Kühne, R., Wagner, P., 2004. Calibration and Validation of Microscopic Traffic Flow Models. Transp. Res. Rec. J. Transp. Res. Board 1876, 62–70.

CARRS-Q, 2018. Advanced Driving Simulator. CARRS-Q.

Chen, D., Ahn, S., Laval, J., Zheng, Z., 2014. On the periodicity of traffic oscillations and capacity drop: The role of driver characteristics. Transp. Res. Part B Methodol. 59, 117–136.

Chen, D., Laval, J.A., Ahn, S., Zheng, Z., 2012. Microscopic traffic hysteresis in traffic oscillations: A behavioral perspective. Transp. Res. Part B Methodol. 46, 1440–1453.

Ciuffo, B.F., Punzo, V., 2010. Verification of Traffic Micro-simulation Model Calibration Procedures: Analysis of Goodness-of-Fit Measures. Presented at the Transportation Research Board 89th Annual Meeting.

Comte, S.L., Jamson, A.H., 2000. Traditional and innovative speed-reducing measures for curves: an investigation of driver behaviour using a driving simulator. Saf. Sci. 36, 137–150.

Dia, H., 2002. An agent-based approach to modelling driver route choice behaviour under the influence of real-time information. Transp. Res. Part C Emerg. Technol. 10, 331–349.

Emami, A., Sarvi, M., Bagloee, S.A., Saberi, M., 2018. Connected Vehicles: An Overview of the Past and Present Developments and Testbeds. Presented at the Transportation Research Board 97th Annual Meeting.

Erke, A., Sagberg, F., Hagman, R., 2007. Effects of route guidance variable message signs (VMS) on driver behaviour. Transp. Res. Part F Traffic Psychol. Behav. 10, 447–457.

Fairclough, S.H., May, A.J., Carter, C., 1997. The effect of time headway feedback on following behaviour. Accid. Anal. Prev. 29, 387–397.

Gao, S., Frejinger, E., Ben-Akiva, M., 2010. Adaptive route choices in risky traffic networks: A prospect theory approach. Transp. Res. Part C Emerg. Technol., Applications of Advanced Technologies in Transportation: Selected papers from the 10th AATT Conference 18, 727–740.

Ge, J.I., Orosz, G., 2014. Dynamics of connected vehicle systems with delayed acceleration feedback. Transp. Res. Part C Emerg. Technol. 46, 46–64.

Ghadiri, S., Prasetijo, J., Sadullah, A., Hoseinpour, M., Sahranavard, S., 2013. Intelligent speed adaptation: Preliminary results of on-road study in Penang, Malaysia. IATSS Res. 36, 106–114.

Greene, D., Liu, J., Reich, J., Hirokawa, Y., Shinagawa, A., Ito, H., Mikami, T., 2011. An Efficient Computational Architecture for a Collision Early-Warning System for Vehicles, Pedestrians, and Bicyclists. IEEE Trans. Intell. Transp. Syst. 12, 942–953.

Groeger, J., 1998. Close, but no cigar: assessment of a headway warning device. Presented at the Automotive Radar and Navigation Techniques (Ref. No. 1998/230), IEE Colloquium on, IET, pp. 5–1.

Guthrie, C., 2002. Prospect Theory, Risk Preference, and the Law Empirical Legal Realism: A New Social Scientific Assessment of Law and Human Behavior. Northwest. Univ. Law Rev. 97, 1115–1164.

Hamdar, S., Treiber, M., Mahmassani, H., Kesting, A., 2008. Modeling driver behavior as sequential risk-taking task. Transp. Res. Rec. J. Transp. Res. Board 208–217.

Hamdar, S.H., Mahmassani, H.S., Treiber, M., 2015. From behavioral psychology to acceleration modeling: Calibration, validation, and exploration of drivers' cognitive and safety parameters in a risk-taking environment. Transp. Res. Part B Methodol. 78, 32–53.

Haque, M.M., Washington, S., 2015. The impact of mobile phone distraction on the braking behaviour of young drivers: a hazard-based duration model. Transp. Res. Part C Emerg. Technol. 50, 13–27.

Hensher, D.A., Rose, J.M., Greene, W.H., 2015. Applied choice analysis, 2nd ed. Cambridge University Press.

Jia, D., Ngoduy, D., 2016. Enhanced cooperative car-following traffic model with the combination of V2V and V2I communication. Transp. Res. Part B Methodol. 90, 172–191.

Jia, H., Gong, S., Yang, D., Li, Y., 2012. Research of Drivers' Car-Following Behavior with Car-Following Suggestion, in: Multimodal Transportation Systems - Convenient, Safe, Cost-Effective, Efficient. Presented at the 12th COTA International Conference of Transportation Professionals, American Society of Civil Engineers, pp. 1223–1234.

John, O.P., Srivastava, S., 1999. The Big Five trait taxonomy: History, measurement, and theoretical perspectives, in: In L. A. Pervin & O. P. John (Eds.), Handbook of Personality: Theory and Research. Guilford Press, New York, pp. 102–138.

Kahneman, D., Tversky, A., 1979. Prospect theory: An analysis of decision under risk. Econom. J. Econom. Soc. 263–291.

Kesting, A., Treiber, M., 2008. Calibrating Car-Following Models by Using Trajectory Data: Methodological Study. Transp. Res. Rec. J. Transp. Res. Board 2088, 148–156.

Kurtc, V., Treiber, M., 2016. Calibrating the Local and Platoon Dynamics of Car-following Models on the Reconstructed NGSIM Data. ArXiv Prepr. ArXiv161003124.

Laval, J.A., 2011. Hysteresis in traffic flow revisited: An improved measurement method. Transp. Res. Part B Methodol. 45, 385–391.

Laval, J.A., Toth, C.S., Zhou, Y., 2014. A parsimonious model for the formation of oscillations in car-following models. Transp. Res. Part B Methodol. 70, 228–238.

Lee, J.D., McGehee, D.V., Brown, T.L., Reyes, M.L., 2002. Collision warning timing, driver distraction, and driver response to imminent rear-end collisions in a high-fidelity driving simulator. Hum. Factors J. Hum. Factors Ergon. Soc. 44, 314–334.

Levy, J.S., 2003. Applications of Prospect Theory to Political Science. Synthese 135, 215–241.

Li, J., Qiu, T., 2018. An Extended Time-Delayed V2X-Based Bidirectional Looking Car-Following Model and Its Linear Stability Analysis. Presented at the Transportation Research Board 97th Annual Meeting Transportation Research Board.

Madsen, M., Gregor, S., 2000. Measuring human-computer trust, in: Proceedings of the 11 Th Australasian Conference on Information Systems. pp. 6–8.

Maltz, M., Shinar, D., 2007. Imperfect in-vehicle collision avoidance warning systems can aid distracted drivers. Transp. Res. Part F Traffic Psychol. Behav. 10, 345–357.

May, A., Carter, C., Smith, F., Fairclough, S., 1995. An evaluation of an in-vehicle headway feedback system with a visual and auditory interface. Presented at the Design of the Driver Interface, IEE Colloquium on, IET, pp. 5–1.

Mittal, A., Mahmassani, H.S., Talebpour, A., 2017. Network Flow Relations and Travel Time Reliability in a Connected Environment. Transp. Res. Rec. J. Transp. Res. Board 2622, 24–37.

Monteil, J., Nantes, A., Billot, R., Sau, J., Faouzi, N. e E., 2014. Microscopic cooperative traffic flow: calibration and simulation based on a next generation simulation dataset. IET Intell. Transp. Syst. 8, 519–525.

NGSIM, 2010. Traffic Analysis Tools: Next Generation Simulation - FHWA Operations [WWW Document]. URL https://ops.fhwa.dot.gov/trafficanalysistools/ngsim.htm (accessed 3.4.17).

Ni, D., Li, J., Andrews, S., Wang, H., 2011. A Methodology to Estimate Capacity Impact due to Connected Vehicle Technology. Int. J. Veh. Technol. 2012.

Ossen, S., Hoogendoorn, S., 2008. Validity of Trajectory-Based Calibration Approach of Car-Following Models in Presence of Measurement Errors. Transp. Res. Rec. J. Transp. Res. Board 2088, 117–125.

Ossen, S., Hoogendoorn, S., 2007. Driver heterogeneity in car following and its impact on modeling traffic dynamics. Transp. Res. Rec. J. Transp. Res. Board 95–103.

Ossen, S., Hoogendoorn, S.P., 2011. Heterogeneity in car-following behavior: Theory and empirics. Transp. Res. Part C Emerg. Technol., Emerging theories in traffic and transportation and methods for transportation planning and operations 19, 182–195.

Punzo, V., Ciuffo, B., Montanino, M., 2012. Can Results of Car-Following Model Calibration Based on Trajectory Data Be Trusted? Transp. Res. Rec. J. Transp. Res. Board 2315, 11–24.

Punzo, V., Montanino, M., 2016. Speed or spacing? Cumulative variables, and convolution of model errors and time in traffic flow models validation and calibration. Transp. Res. Part B Methodol. 91, 21–33.

Punzo, V., Montanino, M., Ciuffo, B., 2015. Do We Really Need to Calibrate All the Parameters? Variance-Based Sensitivity Analysis to Simplify Microscopic Traffic Flow Models. IEEE Trans. Intell. Transp. Syst. 16, 184–193.

Punzo, V., Simonelli, F., 2005. Analysis and Comparison of Microscopic Traffic Flow Models with Real Traffic Microscopic Data. Transp. Res. Rec. J. Transp. Res. Board 1934, 53–63.

Rahman, M.S., Abdel-Aty, M., Wang, L., Lee, J., 2018. Understanding the Highway Safety Benefits of Different Approaches of Connected Vehicles in Reduced Visibility Conditions. Transp. Res. Rec. 0361198118776113.

Ranjitkar, P., Nakatsuji, T., Asano, M., 2004. Performance Evaluation of Microscopic Traffic Flow Models with Test Track Data. Transp. Res. Rec. J. Transp. Res. Board 1876, 90–100.

Saffarian, M., De Winter, J.C., Happee, R., 2013. Enhancing driver car-following performance with a distance and acceleration display. IEEE Trans. Hum.-Mach. Syst. 43, 8–16.

Saifuzzaman, M., Zheng, Z., 2014. Incorporating human-factors in car-following models: A review of recent developments and research needs. Transp. Res. Part C Emerg. Technol. 48, 379–403.

Saifuzzaman, M., Zheng, Z., Mazharul Haque, M., Washington, S., 2015. Revisiting the Task–Capability Interface model for incorporating human factors into car-following models. Transp. Res. Part B Methodol. 82, 1–19.

Sharma, A., Ali, Y., Saifuzzaman, M., Zheng, Z., Haque, M.M., 2017. Human Factors in Modelling Mixed Traffic of Traditional, Connected, and Automated Vehicles, In: Advances in Intelligent Systems and Computing. Presented at the International Conference on Applied Human Factors and Ergonomics, Springer, Cham, pp. 262–273.

Sharma, A., Zheng, Z., Bhaskar, A., 2018a. A pattern recognition algorithm for assessing trajectory completeness. Transp. Res. Part C Emerg. Technol. 96, 432–457.

Sharma, A., Zheng, Z., Bhaskar, A., 2018b. Is more always better? The impact of vehicular trajectory completeness on car-following model calibration and validation. Transp. Res. Part B Methodol. 120C, 49–75.

Summala, H., 1988. Risk control is not risk adjustment: the zero-risk theory of driver behaviour and its implications. Ergonomics 31, 491–506.

Sun, Jie, Zheng, Z., Sun, Jian, 2018. Stability analysis methods and their applicability to car-following models in conventional and connected environments. Transp. Res. Part B Methodol. 109, 212–237.

Talebpour, A., Mahmassani, H., Hamdar, S., 2011. Multiregime Sequential Risk-Taking Model of Car-Following Behavior: Specification, Calibration, and Sensitivity Analysis. Transp. Res. Rec. J. Transp. Res. Board 60–66.

Talebpour, A., Mahmassani, H.S., 2016. Influence of connected and autonomous vehicles on traffic flow stability and throughput. Transp. Res. Part C Emerg. Technol. 71, 143–163.

Talebpour, A., Mahmassani, H.S., Bustamante, F.E., 2016. Modeling Driver Behavior in a Connected Environment. Transp. Res. Rec. J. Transp. Res. Board 2560, 75–86.

Talebpour, A., Mahmassani, H.S., Hamdar, S.H., 2017. Effect of information availability on stability of traffic flow: Percolation theory approach. Transp. Res. Part B Methodol.

Tampere, C.M.J., Hoogendoorn, S.P., Arem, B. van, 2009. Continuous Traffic Flow Modeling of Driver Support Systems in Multiclass Traffic With Intervehicle Communication and Drivers in the Loop. IEEE Trans. Intell. Transp. Syst. 10, 649–657.

Tang, T., Shi, W., Shang, H., Wang, Y., 2014. A new car-following model with consideration of inter-vehicle communication. Nonlinear Dyn. 76, 2017–2023.

Tian, J., Jiang, R., Li, G., Treiber, M., Jia, B., Zhu, C., 2016. Improved 2D intelligent driver model in the framework of three-phase traffic theory simulating synchronized flow and concave growth pattern of traffic oscillations. Transp. Res. Part F Traffic Psychol. Behav. 41, 55–65.

Tian, J., Treiber, M., Ma, S., Jia, B., Zhang, W., 2015. Microscopic driving theory with oscillatory congested states: Model and empirical verification. Transp. Res. Part B Methodol. 71, 138–157.

Train, K.E., 2009. Discrete choice methods with simulation, 2nd ed. Cambridge University Press.

Treiber, M., Hennecke, A., Helbing, D., 2000. Congested traffic states in empirical observations and microscopic simulations. Phys. Rev. E 62, 1805.

Treiber, M., Kesting, A., 2013a. Microscopic Calibration and Validation of Car-Following Models – A Systematic Approach. Procedia - Soc. Behav. Sci., 20th International Symposium on Transportation and Traffic Theory (ISTTT 2013) 80, 922–939.

Treiber, M., Kesting, A., 2013b. Traffic flow dynamics. Traffic Flow Dyn. Data Models Simul. Springer-Verl. Berl. Heidelb.

Treiber, M., Kesting, A., Helbing, D., 2006. Understanding widely scattered traffic flows, the capacity drop, and platoons as effects of variance-driven time gaps. Phys. Rev. E 74, 016123.

von Neumann, J., Morgenstern, O., 1944. Theory of Games and Economic Behavior. Princet. Univ. Press.

Wallace, W.A., 1996. The modeling of nature: philosophy of science and philosophy of nature in synthesis. Catholic University of America Press.

Weisberg, M., 2013. Simulation and Similarity: Using Models to Understand the World. Oxford University Press.

Xu, H., Zhou, J., Xu, W., 2011. A decision-making rule for modeling travelers' route choice behavior based on cumulative prospect theory. Transp. Res. Part C Emerg. Technol., 19, 218–228.

Yang, J., Jiang, G., 2014. Development of an enhanced route choice model based on cumulative prospect theory. Transp. Res. Part C Emerg. Technol., 47, 168–178.

Zheng, Z., 2014. Recent developments and research needs in modeling lane changing. Transp. Res. Part B Methodol. 60, 16–32.

Zheng, Z., Ahn, S., Chen, D., Laval, J., 2011a. Freeway traffic oscillations: Microscopic analysis of formations and propagations using Wavelet Transform. Transp. Res. Part B Methodol., 45, 1378–1388.

Zheng, Z., Ahn, S., Chen, D., Laval, J., 2011b. Applications of wavelet transform for analysis of freeway traffic: Bottlenecks, transient traffic, and traffic oscillations. Transp. Res. Part B Methodol. 45, 372–384.

Zhu, F., Ukkusuri, S.V., 2017. Modeling the Proactive Driving Behavior of Connected Vehicles: A Cell-Based Simulation Approach. Comput.-Aided Civ. Infrastruct. Eng. 33, 262–281.